LAPPEENRANTA-LAHTI UNIVERSITY OF TECHNOLOGY LUT
School of Energy Systems
Electrical Engineering
Master's Thesis
2019

Katriina Korpinen

A STUDY ON THE FIELD FAILURES OF CERTAIN DIODE BRIDGE RECTIFIERS

Examiners: Professor Pertti Silventoinen
D.Sc. Tommi Kärkkäinen

Abstract

Katriina Korpinen

A Study on the Field Failures of Certain Diode Bridge Rectifiers

Master's Thesis

Lappeenranta 2019

55 pages

Examiners: Professor Pertti Silventoinen and D.Sc. Tommi Kärkkäinen

Keywords: diode, rectifier, breakdown, imaging methods, X-ray imaging

A power supply manufacturer had experienced field failures of three-phase diode bridge rectifier modules. The modules seemed to lose their ability to withstand voltage. In this thesis, the rectifier modules used by the power supply manufacturer were studied. The power supply manufacturer delivered a total of 35 unused rectifier modules and 50 used field returns. The modules were of three different case types. The objectives of the study were to detect any differences in breakdown voltages or in structure between the case types and to identify possible failure mechanisms of the breakdown.

The breakdown voltages of the diodes were measured with a power device analyzer and the internal structure was examined using 2D and 3D X-ray imaging, cross sectioning, an optical microscope, a scanning electron microscope (SEM) and energy-dispersive X-ray spectroscopy (EDS). Multiple differences were discovered. Case type 3 modules had clearly the highest breakdown voltage values. Case types 1 and 2 had lower breakdown voltage values and they also had problems like permanent breakdowns and gradually decreasing breakdown voltages. Three distinctly different internal structures were discovered and also the chemical composition had differences between the three case types. The cross sectioning also revealed cracks and heat damage in some case type 1 and 2 diodes. In conclusion, it could be stated that there has been some significant imperfections with the layout or with the manufacturing process of case type 1 and 2 rectifier modules.

Tiivistelmä

Katriina Korpinen

Tutkimus tiettyjen diodisiltatasasuuntaajien vikaantumisista kentällä

Diplomityö

Lappeenranta 2019

55 sivua

Työn tarkastajat: Professori Pertti Silventoinen ja TkT Tommi Kärkkäinen

Avainsanat: diodi, tasasuuntaaja, läpilyönti, kuvantamismenetelmät, röntgenkuvaus

Eräs teholähdevalmistaja oli kokenut diodisiltatasasuuntaajien vikaantumisia kentällä. Tasasuuntaajat menettivät jännitekestonsa. Tässä diplomityössä tutkittiin teholähdevalmistajan käyttämiä tasasuuntaajamoduuleja. Teholähdevalmistaja toimitti yhteensä 35 käyttämätöntä tasasuuntaajaa ja 50 käytettyä kentältä palautettua tasasuuntaajaa. Tasasuuntaajissa oli kolmea erilaista kotelointitapaa. Tutkimuksen tavoitteena oli löytää mahdolliset erot kotelointitapojen läpilyöntijännitteissä ja rakenteessa, sekä tunnistaa läpilyöntiin johtavat vikaantumismekanismit.

Diodien läpilyöntijännitteet mitattiin puolijohdeanalysaattorilla ja tasasuuntaajamodulien rakennetta tutkittiin 2D- ja 3D-röntgenlaitteilla, poikkileikkaamalla, optisella mikroskoopilla, pyyhkäisyelektronimikroskoopilla (SEM) ja energiadispersiivisellä röntgenspektrometrillä (EDS). Kotelointitavoilla 1 ja 2 oli selvästi alhaisemmat läpilyöntijännitteet kuin kotelointitapa 3:lla. Kotelointitavoissa 1 ja 2 havaittiin myös lievästi alenevia läpilyöntijännitteitä sekä peruuttamattomia läpilyöntejä, jotka tiputtivat läpilyöntijännitteen kerralla alle kymmenekseen edellisestä mittauksesta. Kotelointitavat edustivat kolmea selvästi erilaista rakennetta ja myös kemiallisessa koostumuksessa oli eroja kotelointitapojen välillä. Poikkileikkaukset paljastivat rakenteellisten erojen lisäksi halkeamia ja lämpövaurioita joissakin kotelointitapojen 1 ja 2 diodeissa. Yhteenvetona voidaan todeta, että kotelointitapojen 1 ja 2 tasasuuntaajamoduulien rakenteessa tai valmistusprosessissa on ollut joitakin merkittäviä puutteita, jotka ovat vaikuttaneet tasasuuntaajien kestävyyteen.

Preface

This study was carried out in the Laboratory of Applied Electronics at LUT University in 2019. I would like to thank Professor Pertti Silventoinen and D.Sc. Tommi Kärkkäinen for providing guidance during this study. I would also like to thank Antti Heikkinen from LUT Voima, Toni Väkiparta and Tuomas Nevalainen from LUT School of Engineering Science and Jonny Ingman from ABB for helping me with the research. And for leading me to this interesting subject and for delivering me the rectifiers, I would like to thank Powernet.

Special thanks to everyone at room 6405 for the coffee breaks and card games that helped me reset my brain during the writing process.

Finally, the biggest thanks must go to my family and especially to my boyfriend, Harri, for all the support throughout my life.

Katriina Korpinen

August 23, 2019

Lappeenranta

Table of Contents

Abstract

Tiivistelmä

Preface

Table of Contents

Nomenclature

1 Introduction 8
1.1 Research problem and research questions 9

2 Research methods 10

3 Possible failure mechanisms in diode bridge rectifiers 13
3.1 Dielectric properties and breakdown 14
3.2 PIN-junction failure 18

4 Measurement and imaging options for diode bridge rectifier modules 19
4.1 Electrical measurements 19
4.2 X-ray imaging 20
4.3 Cross sectioning and observing with an optical microscope 21
4.4 Scanning electron microscope (SEM) and energy-dispersive X-ray spectroscopy (EDS) 21
4.5 Lock-in Thermography (LIT) 22
4.6 Acoustic imaging 22

5 Diode breakdown voltage measurements 23

6 Examining the structure and materials of the modules 29
6.1 Possible materials inside the modules 29
6.2 X-ray imaging 30
6.3 Destructive methods 33
6.4 The chemical elements in the rectifier modules 40

7 Conclusions and discussion 45

References 48

Appendices

Appendix 1: The difference between the first and the last breakdown voltage measurement result for each diode in the new unused rectifier modules.

Appendix 2: The difference between the first and the last breakdown voltage measurement result for each diode in the unused field returned rectifier modules.

Nomenclature

U_{br}	[V]	breakdown voltage
U_{RRM}	[V]	repetitive peak reverse voltage

AC	alternating current
ASD	adjustable-speed drives
CT	computed tomography
DC	direct current
EDS	energy-dispersive X-ray spectroscopy
HVDC	high-voltage direct current
SEM	scanning electron microscope
SMPS	switched-mode power supply

1 Introduction

The era of power electronics began in 1902 when Peter Cooper Hewitt invented the rectifier. It was a mercury-arc rectifier designed to convert alternating current (AC) to direct current (DC) for a motor. (Guarnieri, 2018) Nowadays rectifiers are mainly semiconductor-based diode bridge modules. Single-phase rectifiers have four diodes per module and three-phase rectifiers have six diodes per module (Figure 1.1). The most common application for diode bridge rectifiers are power supplies, frequency converters and high-voltage direct current (HVDC) electric power transmission systems. Frequency converters are commonly found in the industry and in electric vehicles. They are used for example in adjustable-speed drives (ASD) to supply electric motors with a desired AC voltage and frequency. (Rashid, 2018) AC-to-DC and switched-mode power supplies (SMPS) are not only common in the industry, but also in homes. Many common household devices need DC for operation, but are supplied from the AC network, so a power supply with diode bridge rectifiers is needed (CDA, 2019).

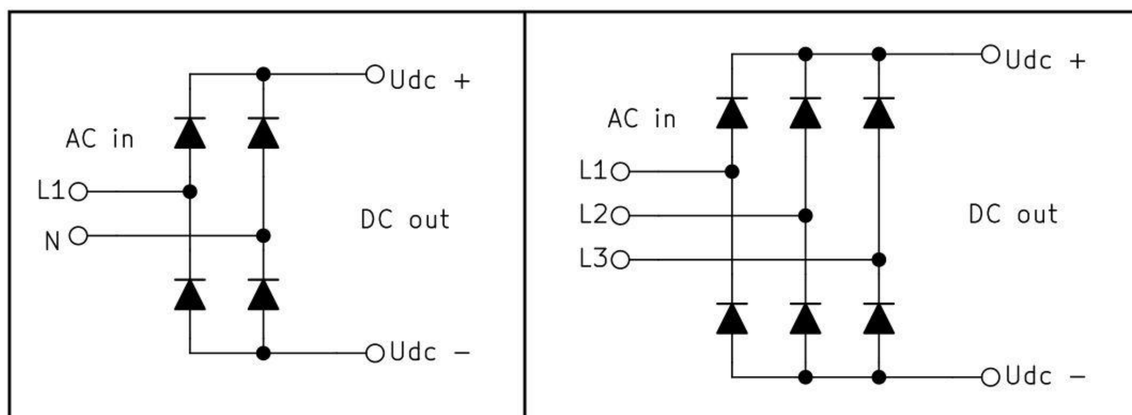

Figure 1.1. Circuit diagrams of a single-phase diode bridge rectifier (on the left) and a three-phase diode bridge rectifier (on the right).

All of the power supplied to the device by the power supply or frequency converter goes through the diodes. The diode bridge structure and diode thickness define how much voltage and current the diode can handle. The diode bridge needs to be suitable for the application. (Rashid, 2018) The diodes also have to be able to withstand the possible fluctuation of the grid and reverse voltage from the device supplied by the frequency converter or power supply.

1.1 Research problem and research questions

A power supply manufacturer had experienced field failures of three-phase diode bridge rectifier modules. The goal of this thesis is to examine the structure of the diode bridge rectifier modules used by the power supply manufacturer and to identify the possible failure mechanisms taking place in the modules. Understanding the phenomenon taking place inside the rectifier bridges and knowing the root cause allows mitigating the problem in the future.

For an unknown reason, the rectifier modules had been losing their ability to withstand voltage despite having a good marginal between the operating voltage and the rated maximum voltage. The breakdown voltages of diodes in the rectifiers had decreased gradually and permanently when the rectifiers were being used. The deterioration of the rectifier modules had caused malfunctions to the power devices. The reasons behind the phenomena of rectifier deterioration and breakdown were unknown.

The main research questions of this thesis are:

- What is the structure of the diode bridge rectifiers?
- Are there significant differences in breakdown voltages or in structure between the rectifier modules?
- What are the failure mechanisms of the breakdown?

2 Research methods

The power supply manufacturer supplied the diode bridge rectifier modules used in the research. The power supply manufacturer had used modules from two different component manufacturers, Diotec and Ixys. Modules from both of these component manufacturers were examined in the research. The modules were chosen so that there was a broad selection of both new unused and used modules from different batches. The used modules were taken from field returns that were either malfunctioning or brought in for service or updates.

The modules in the research consisted of three different case types that are presented in Figure 2.1. The case types were classified according to the way they were labeled and how the prints were placed on the cases. From Diotec there were two case types (case type 1 and case type 2) and from Ixys there was one case type (case type 3). On case type 1 the model number was on the top of the side of the case and the batch number was on the right half printed in one row. On case type 2 the model number was also on the top of the side of the case, but the batch number on the right half was printed in two rows. On case type 3 the model number was on the bottom left corner of the side of the case and the batch number was on the right half printed in two rows.

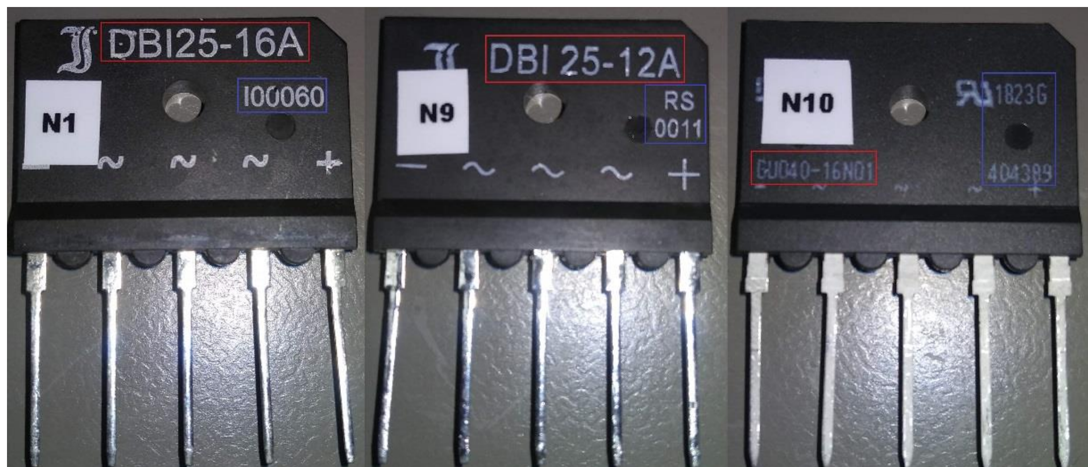

Figure 2.1. Three case types with different labeling layouts were recognized. Case type 1 is on the left, case type 2 in the middle and case type 3 on the right. Model names are marked with red and batch numbers with blue.

The modules studied in this research were delivered by the power device manufacturer in two batches. The first batch included 15 unused and 6 used diode bridge rectifiers. All of the used rectifiers were of case type 1 or 2, because there weren't any used case type 3 modules available. Case type 3 rectifiers from Ixys had been used by the power device manufacturer for only a short period of time and there hadn't yet been any issues with their ability to withstand voltage. The second batch of diode bridge modules delivered by the power device manufacturer included 20 unused and 44 used modules. The second batch had used and unused modules of all three case types. The total amounts of received rectifier modules of each case type are presented in Table 2.1.

Table 2.1. The research material included new and used diode bridge rectifier modules of three case types. The rectifier modules were from two manufacturers.

	Case type 1	Case type 2	Case type 3
New, unused [pcs]	12	7	16
Used, field returns [pcs]	18	30	2
Manufacturer	Diotec	Diotec	Ixys

The used modules of the first batch had already been named and marked by the power device manufacturer. The same method of naming was used for the rest of the modules as well. The modules were named depending on whether they were new unused modules or used modules from returned devices. The new unused modules were named "N" plus a running number and the used field returns were named "R" plus a running number (Table 2.2). The names of the modules were marked to each module using tape (Figure 2.1).

Table 2.2. Naming method of the rectifier modules.

	Letter	Number	Example
New, unused	N	1-35	N12
Used, field returns	R	11-66	R45

A substantial part of the research was experimental, but also some literature study was carried out. The literature study focused on finding out possible failure mechanisms of diode bridge modules and getting acquainted with dielectric breakthrough mechanisms.

The literature study helped identify the possible failure mechanisms in the examined modules.

The experimental research consisted of measuring the breakdown voltages and examining the internal structure of the modules. The breakdown voltage measurements were carried out using a power device analyzer and curve tracer. All diodes from all modules were measures separately at least three times. The reverse voltage supplied by the power device analyzer was increased up from 0 V to 3000 V in roughly 10 V steps. The measurement was stopped when the reverse current rose to over 30 µA. The breakdown voltage was taken to be the voltage where the reverse current was roughly 10 µA.

The internal structure was examined using multiple methods. All of the first batch modules and some second batch modules were 2D X-ray imaged to get a basic understanding of the internal structure. Furthermore, multiple methods were used to get an even better understanding of the internal structure of the modules. Different chemicals and melting were tried out for removing the epoxy case. A wet disc cutter was used to cut some modules in half to see the cross section. The cross sections were examined using an optical microscope and a scanning electron microscope (SEM). Energy-dispersive X-ray spectroscopy (EDS) was utilized to identify the chemical elements present. Later also an opportunity for 3D X-ray imaging occurred and the internal structure could be examined even more precisely.

3 Possible failure mechanisms in diode bridge rectifiers

A breakdown in a diode bridge rectifier module can happen either inside the diode itself or between conducting parts through the dielectric. The structure of the conducting parts and placement of the diodes inside the module are presented in Figure 3.1. Before a full breakdown and short circuit, it is possible to get slightly deteriorated performance values.

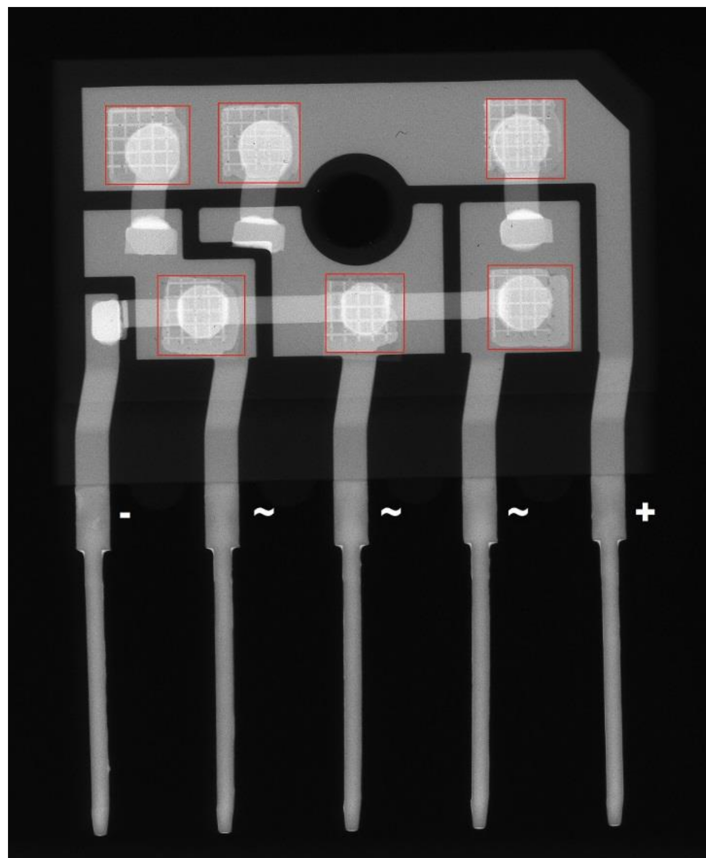

Figure 3.1. X-ray image of case type 1 structure. All three case types had similar structure with three diodes on the top row and three on the bottom row (diodes marked with red squares). The pin layout was also same for all three case types with the minus pin on the left, plus pin on the right and three phase pins in the middle.

The basic structure was the same for all three case types with six diodes in two rows and with narrow conducting rails connecting the diodes from above and bigger conducting plates connecting the diodes from below as shown in Figure 2.1. However, the conducting parts were shaped slightly differently and there were differences in how the

diodes were attached. Case type 1 had a mesh pattern engraved to the copper parts around the diode, case type 2 had the diodes simply soldered between two copper plates and case type 3 had the most complex structure with multiple copper parts above the diodes.

3.1 Dielectric properties and breakdown

The dielectric case material in the studied diode bridge rectifiers is cured epoxy (Diotec Semiconductor AG, 2017; IXYS, 2016; IXYS, 2013). Epoxies in general have good electrical insulation properties, temperature resistance and mechanical durability, and therefore they are widely used in electronics and electrical systems (Klampar et al., 2013). Epoxies are used for example for sealing, coating, bonding and encapsulating. The properties of epoxy depend especially on the curing agent used to harden the epoxy resin. The choice of curing agent affects insulation properties, operational temperatures, physical strength and chemical resistance of the epoxy. (Tech Briefs Media Group, 2014)

Some of the most important insulation properties are the dielectric constant, the dielectric losses, the dielectric strength and volume resistivity (Guo et al., 2018; Song et al., 2014; Heid et al., 2013). The dielectric constant is also known as relative permittivity. It is used to describe how much electrical energy is stored to the material when a voltage is applied. The dielectric constant decreases when the frequency of the applied voltage is higher. (Bernard & Gautray, 1991) A low dielectric constant is preferred for insulators and for example the epoxy-silica nanocomposites studied by Veena (2012) had a dielectric constant varying from 3,2 to 3,9 (Veena et al., 2012).

The dielectric losses describe the power losses in a material when an alternating electric field is applied. The dielectric losses increases when frequency increases. Temperature also affects the dielectric losses. Low dielectric losses are preferred since heating the insulation material is not desired. (Guo et al., 2018) The dielectric losses can change over time due to voids, moisture, contamination and severe operational conditions (Tech Briefs Media Group, 2014).

Volume resistivity describes the ability to resist current from flowing through the material. Ideally, volume resistivity of an insulator is large (Heid et al., 2013). Heat reduces volume resistivity, but it is not permanent unless the heat damages the material (Zavattoni et al., 2013).

The dielectric strength is the maximum electric field strength that can be applied over one thickness unit of the material without causing a dielectric breakdown. The breakdown voltage depends on the thickness of the material and the dielectric strength can be calculated by dividing he breakdown voltage with the thickness of the material. (Song et al., 2014) For example air has a dielectric strength of 3,0 kV/mm and epoxy can have a dielectric strength of above 30 kV/mm (Tipler, 1987).

Dielectric breakdown is the phenomenon of an insulator becoming conductive. In dielectric breakdown, the resistance of the material rapidly decreases allowing current to flow through it (Tech Briefs Media Group, 2014). This usually happens if the voltage over the material is higher than the dielectric strength. Unlike gases and liquids, solid dielectrics get permanently damaged in an electrical breakdown. (E. M. S., 2014)

There are multiple different types of breakdown mechanisms for a dielectric breakdown such as intrinsic breakdown, electrochemical breakdown, thermal breakdown and mechanical breakdown. Also partial discharges and treeing can lead to breakdown (E. M. S., 2014). For example temperature, moisture, impurities, voltage and time affect the breakdown mechanism that will take place.

An intrinsic breakdown happens in tens of nanoseconds and is caused by conduction electrons in the dielectric. There are two types of mechanisms for freeing more electrons to conduction band. One mechanism is that the applied voltage and electric field causes electrons to jump from valence band to conduction band and the large number of conduction electrons eventually leads to breakdown. The other mechanism is that conduction electrons collide to lattice atoms and the collisions free more electrons to conduction band. (E. M. S., 2014) In a dielectric material the band gap between valence band and conduction band is the biggest. Semiconductors have a small band gap and

conductors, for example metals, have no band gap (Figure 3.2). The bigger the band gap, the more energy is needed to free the electrons. (Semiconductor Technology, 2019)

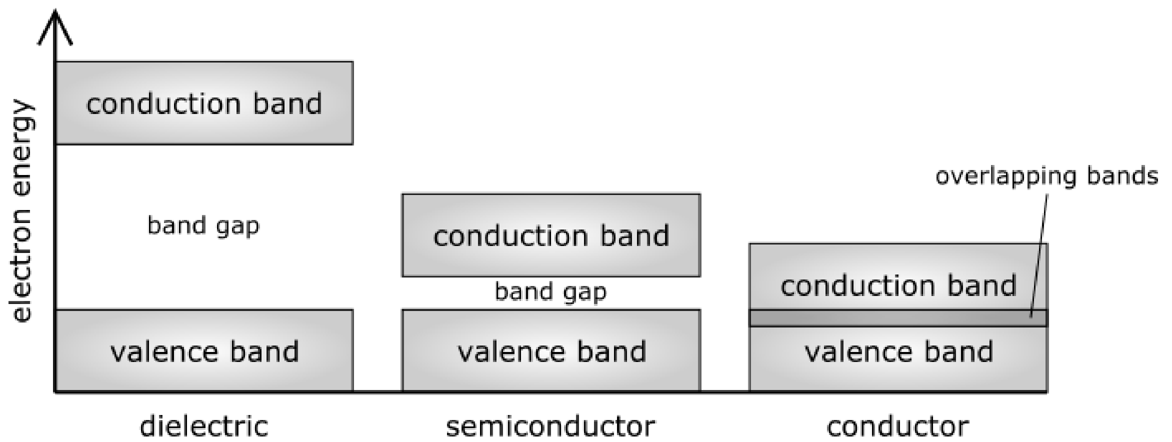

Figure 3.2. The band gap between valence band and conduction band is the biggest for insulators. In an intrinsic breakdown electrons jump from valence band to conduction band and energy is required.

Thermal breakdown happens when the generated heat exceeds the dissipated heat. There is always some current flowing through even a dielectric. The current generates heat. The dissipated heat consists of the heat used to warm up the dielectric and the heat radiated to the surroundings. (E. M. S., 2014) There are at least two types of thermal breakdown. One is that the temperature increase causes physical changes, such as meltdown, in the dielectric. The other is that the excess heat causes electron movement and thus leads to conductivity and breakdown. (Champion et al., 2001)

Treeing is the process of gas filled dendrites developing inside an insulator material. Treeing can be caused by partial discharges inside the insulation. Partial discharges occur because of voids and impurities mainly at junctions. The partial discharges char and erode the dielectric forming a treelike conductive path through the dielectric. (E. M. S., 2014) There are at least three different tree types that have been recognized: the initial dark tree, the filamentary tree and the reverse tree. An initial dark tree is a short and thick tree that usually appears first. Filamentary treeing can develop subsequent to the initial dark tree (Figure 3.3) or on its own without an initial dark tree. A filamentary tree has very thin branches and it doesn’t affect the insulator properties radically. Zheng et al. (2017) claim that filamentary trees might be caused, unlike the other tree types, by

an electromechanical process rather than partial discharges. A reverse tree can start to grow when the filamentary tree has grown all the way through the dielectric. A reverse tree has thicker branches and can eventually lead to dielectric breakdown as shown in Figure 3.3. (Zheng et al., 2017)

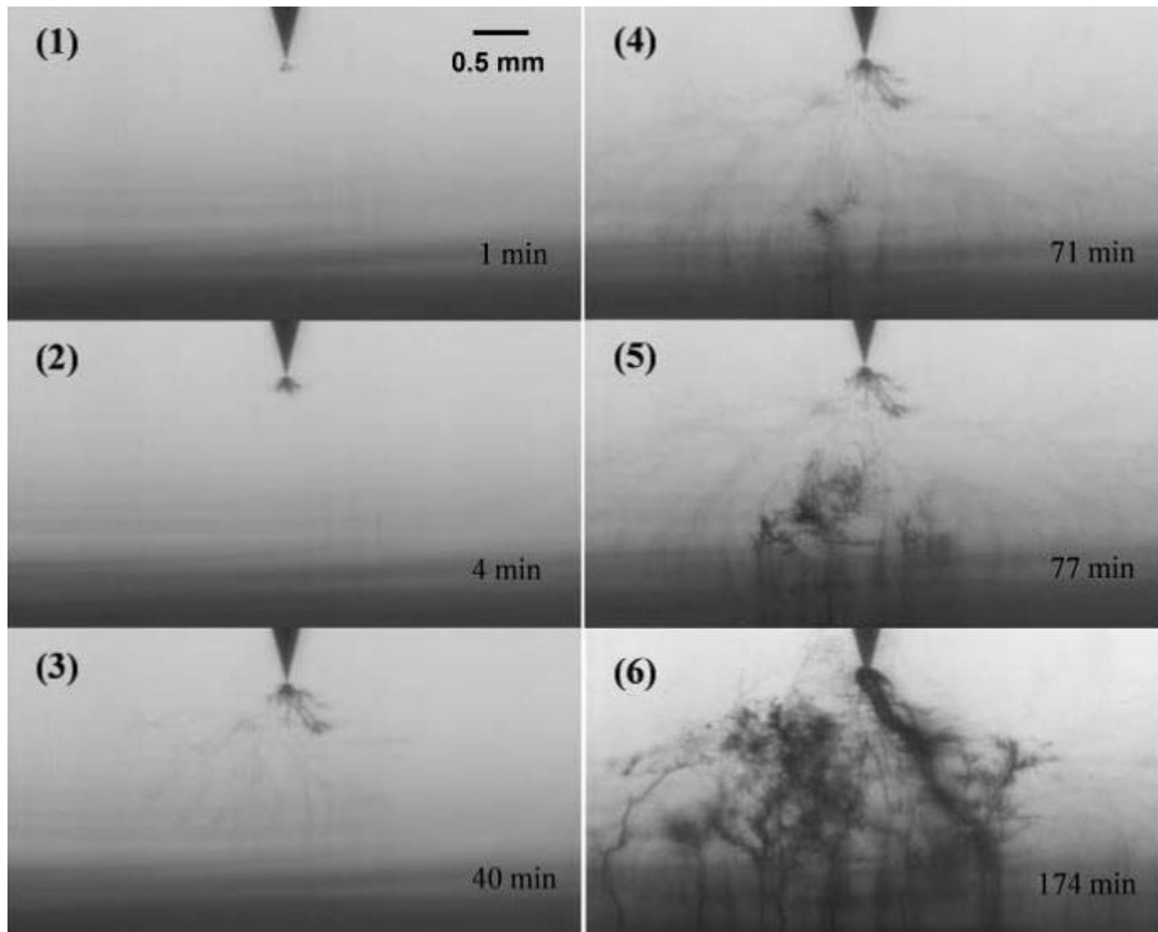

Figure 3.3. The process of treeing in an insulator from a needle electrode tip to electrode plane. Pictures (1) and (2) show a dark and thick initial dark tree developing. In picture (3) the thin filamentary treeing has started to spread. The reverse tree growth can be seen in pictures (4) and (5). This test in question resulted in breakdown as shown in picture (6). (Zheng et al., 2017)

Electrochemical deterioration such as oxidation and hydrolysis lead to weakening of the dielectric properties and can eventually cause breakdown. Also ion migration and metallic dendrites can be considered as an electrochemical process. (EEEGUIDE, 2019)

Finally, also electromechanical and mechanical stress can cause dielectric breakdown. The forces of an electric field or external pressure or impact can cause fractures, cracks

and fragility to the dielectric and thus lead to breakdown. (E. M. S., 2014)

3.2 PIN-junction failure

PIN-junctions, also referred to as diodes, are these days most commonly constructed from silicon. The silicon chip conducts current from anode to cathode when a forward biased voltage is applied. A small reverse current from cathode to anode is unwanted but inevitable.

If a reverse bias higher than the breakdown voltage is applied to a diode, breakdown happens and the diode becomes conductive from cathode to anode. Breakdown is usually not desired, since high reverse currents can break the diode easily (Obreja et al., 2005). Only Zener and transient voltage suppressor diodes are used intentionally reverse biased operating in the breakdown region (Obreja et al., 2010). Diodes can recover from breakdown and the breakdown itself will not damage the diode. However, the reverse current can cause heat and permanent damage (Obreja et al., 2005).

Heat can be caused by reverse current, too much current or uneven current. Uneven current occurs when a silicon chip conducts better from some parts than others. This causes local hotspots. (Obreja et al., 2005) Heat can also be conducted from outside or from nearby devices or components. Bad cooling or poor heat transfer can also be the cause for excessive heat. In example voids reduce the effective heat transfer surface from the silicon chip and can thus cause heat damage (Wang et al., 2018).

Mechanical stress can also cause diode failure. Mechanical stress can be for example vibrations, hits, stretch or pressure. Mechanical stress leads to cracks. The manufacturing process of the modules can cause stress or stress can occur in use. Vibration can be caused for example by industrial machines or motors. Stretch and pressure can be caused by heat expansion. (Qamar et al., 2014) The cracks caused by mechanical stress lower the breakdown voltage significantly and conduct current in both directions. They also cause hot spots.

4 Measurement and imaging options for diode bridge rectifier modules

Nowadays a wide range of options for measuring and imaging components are available. All methods have their strengths and weaknesses. Using a combination of multiple methods enables to get a more precise understanding of the structure and properties of the component.

4.1 Electrical measurements

Electrical measurements can be used to examine the electrical properties of a rectifier module. This method is mainly non-destructive, but it doesn't provide any information about the structure of the module. Electrical measurements can be used to see if the modules meet the values provided by the datasheet. All of the modules should easily be able to withstand the maximum operational conditions provided by the datasheet. Tests can be also done outside the datasheet maximum operational values to find differences between modules. For example, breakdown voltages of each diode can be measured, but it should be noted that it is impossible to tell if the breakdown actually happened in the diode or if it happened through some dielectric material or from the edge of the diode.

Power device analyzers with curve tracer properties can be used to measure the properties of diode bridge rectifier modules. For example the Keysight B1505A Power Device Analyzer / Curve Tracer can be used to measure the forward characteristics of each diode, the leakage currents of each diode and it can also be used to measure the absolute breakdown voltages of the diodes. The leakage current is most often measured until the datasheet repetitive peak reverse voltage provided by the datasheet. The absolute breakdown voltage can be measured by sweeping the voltage up in steps and measuring the leakage current until the breakdown happens. The Keysight instrument can automatically give the results in a graph as shown in Figure 4.1. When the range of operation is from -3000 V to 3000 V and from -4 mA to 4 mA, the measurement resolution is 200 µV and 10 fA. (Keysight Technologies, 2019)

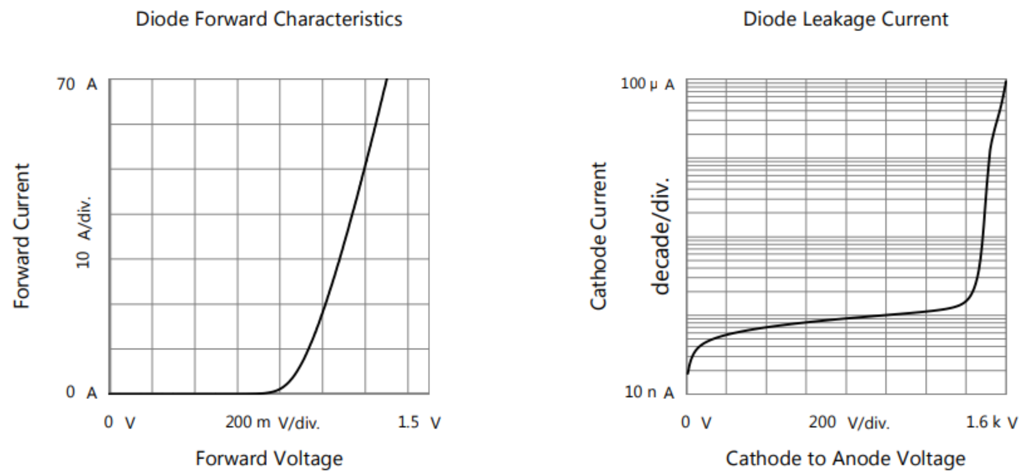

Figure 4.1. Electrical measurements of a diode in rectifier module R17. The measurements were done with the Keysight B1505A Power Device Analyzer / Curve Tracer. On the left is the diode forward characteristics graph and on the right is the diode leakage current graph. According to the datasheet the leakage current was supposed to be less than 5 µA at the repetitive peak reverse voltage 1600 V (Keysight Technologies, 2019).

4.2 X-ray imaging

X-ray imaging is another non-destructive method of imaging internal structures. X-ray imaging uses radiation of mainly wavelengths ranging from 2 to 14 nm to create the image (Artyukov et al., 2018). These X-rays can penetrate nearly all materials (Semmens, 2019). The material affects how dark or light the structures appear in the image. Internal structures with a higher mass density appear lighter in the image whereas the structures with a smaller mass density appear darker.

X-ray imaging can be used to see the big picture and to get a basic idea of the internal structures of for example a diode bridge rectifier. X-ray imaging is especially good for imaging metal structures that are inside plastic, because X-rays can easily penetrate plastics. (Semmens, 2019)

With 2D X-ray technologies it is possible to see non-contact opens, big voids and distinct misalignments (Sylvester et al., 2013). However, small gaps or delaminations might not be recognized unless the X-ray angle is perfect (Semmens, 2019). With 3D X-ray technologies, such as laminography and computed tomography (CT), it is

possible to get a much higher resolution and therefore it is also possible to see smaller voids and delaminations (Sylvester et al., 2013).

4.3 Cross sectioning and observing with an optical microscope

Cross sectioning is a destructive method. The components, for example rectifier modules, can be cut in half with for example a wet disc cutter. After cutting, the cross section surface has to ground to desired spot and polished to eliminate any scratches or impurities. Before these operations the components can be molded into hard epoxy to give them support.

The polished surface can then be observed with an optical microscope. An optical microscope has the same basic principle as an ordinary magnifying glass. It uses objective lenses and light to magnify the image.

This method is not very useful on its own, because it only reveals one slice of the internal structure. Especially when trying to find voids, cracks or other anomalies, this method is pretty much a hit-and-miss. When combined with other imaging methods like X-ray imaging, cross sectioning and an optical microscope can be very useful.

4.4 Scanning electron microscope (SEM) and energy-dispersive X-ray spectroscopy (EDS)

A scanning electron microscope (SEM) can also be used to magnify and observe the cross section of a component. A SEM doesn’t use objective lenses for the magnification like a regular optical microscope does. A SEM produces a beam of electrons, scans the surface of the specimen and gathers the secondary electrons with a detector. The SEM image can have a magnification from 25x up to 1000000x and it is a black and white image. (Liu et al., 2016)

A SEM can also be used to examine the elemental composition of the specimen. This is possible by using energy-dispersive X-ray spectroscopy (EDS) analysis. EDS analysis utilizes the fact that each chemical element has their own unique atomic structure and

electromagnetic emission spectrum. With EDS mapping it is possible to find out all the chemical elements and their locations in a cross section surface. (National Technical Systems, 2019)

4.5 Lock-in Thermography (LIT)

Lock-in thermography (LIT) is a non-destructive method that can be used for characterization of materials (Pham Tu Quoc, 2013). In LIT, the surface of the sample is heated with a repetitive rate light source like a halogen lamp. The thermal waves reflect at boundaries inside the sample and affect the infrared radiation that is emitted from the sample. The emitted infrared radiation from the sample is then measured with an infrared camera. By knowing the phase and amplitude of the repetitive rate light source and the emitted infrared radiation, defects can be located. (Meola, 2007)

LIT can also be used for finding hotspots by using the sample itself as the source of heat. When using this method, the lock-in signal of a certain frequency is used for pulsating the input voltage. This method has been used for finding failures in multilayer ceramic capacitors and tantalum capacitors. (Andersson et al., 2018)

4.6 Acoustic imaging

Similarly to LIT, acoustic methods can also be used for detecting micro-cracks, delamination or small air gaps in components. A scanning acoustic microscope uses ultrasound frequencies between 5 and 500 MHz. The ultrasonic waves reflect from the different structures and acoustic impedances inside the component and the internal structure can be imaged. (Semmens, 2019) Acoustic imaging is good for detecting air-filled pockets or cracks, because the acoustic impedance of air is so much smaller than that of for example plastics or metals. On the other hand, metallic structures are harder to image using acoustic imaging and X-ray imaging is much more accurate for them. (Barth et al., 2008)

5 Diode breakdown voltage measurements

The modules were measured with a Keysight B1505A Power Device Analyzer / Curve Tracer. A voltage sweep was used to find the breakdown voltages U_{br} for each diode. The analyzer was set to increase the voltage in 10 V steps from 0 V to 3000 V. Current was measured after each step and a stop condition was set to 30 µA. The measurement time was 10 µs and the step time was 500 µs. The analyzer was able to stop the measurement and cut off the voltage every time before the current could reach 200 µA. A current-voltage curve of a desirably working diode is shown in Figure 5.1.

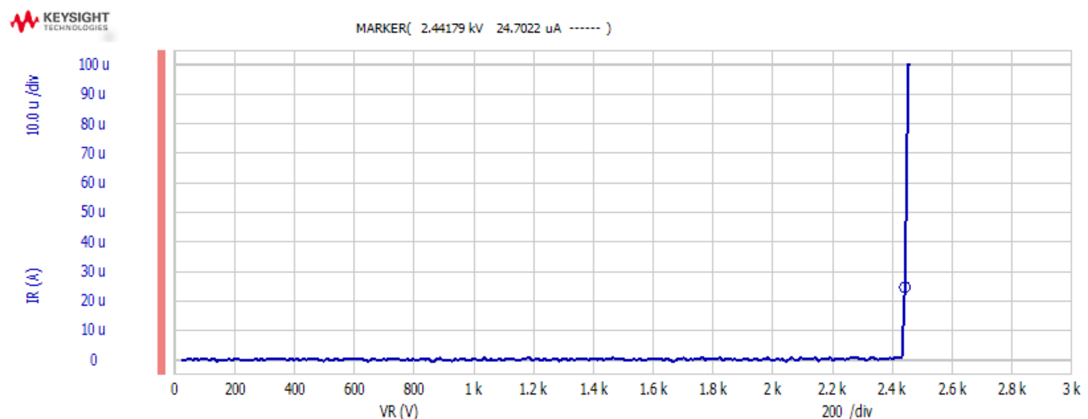

Figure 5.1. Diode working as expected. Breakdown and rapid rise of the reverse current happens at 2440 V.

According to the rectifier module datasheets, the repetitive peak reverse voltage U_{RRM} was 1600 V per diode for all case type 1 and most case type 2 and 3 modules (Diotec Semiconductor AG, 2017; IXYS, 2016; IXYS, 2013). The maximum output currents and maximum forward surge currents were similar for all modules with only small differences (Table 5.1). The leakage current, when the reverse voltage was set to U_{RRM}, was 40 µA for the Ixys modules and less than 5 µA for the Diotec modules. (Diotec Semiconductor AG, 2017; IXYS, 2016; IXYS, 2013) The characteristics are shown in Table 5.1.

Table 5.1. Characteristics of the rectifier modules.

	Case type 1	Case type 2	Case type 3
repetitive peak reverse voltage	1600 V	16A modules: 1600 V 12A modules: 1200 V	GUO40-16NO1 modules: 1600 V DNA40U2200GU modules: 2200
maximum output current	40 A at 85 °C	40 A at 85 °C	40 A at 90 °C
maximum forward surge current	370 A at 25 °C	370 A at 25 °C	370 A at 45 °C
leakage current	< 5 µA	< 5 µA	40 µA

The breakdown voltage of each diode was measured at least three times with the power device analyzer. A total of 35 new unused modules and 50 used field returns were measured. Most diodes had a stabile breakdown voltage value with a maximum of 30 V difference between the consecutive measurements, but some modules had diodes that showed a big decrease, slight decrease or slight increase in the values of subsequent measurements. The results by case type have been gathered to Table 5.2 and the results of all individual diodes are presented in Appendices 1 and 2.

Table 5.2. All diodes were measured at least three times. Most diodes had a stabile breakdown voltage value between the consecutive measurements, but some modules had diodes that experiences a big decrease, slight decrease or slight increase of the breakdown voltage value. The results by case type are presented in this table.

	Case type 1	Case type 2	Case type 3	All modules
Total number of modules	30	37	18	85
Big decrease (>1000 V decrease, or to less than one tenth of previous measurement)	10	4	0	14
Slight decrease (>30 V decrease)	1	26	0	27
Slight increase (>30 V increase)	3	8	0	11
Stabile value (all measurements within 30 V from each other)	18	7	18	43

Case type 1 had steady values in 60 % of modules and case type 2 had steady values in only 19 % of modules. Case type 3 showed steady values consistently with all of the diodes having a maximum of 20 V difference between the consecutive measurements.

Some diodes got permanently damaged in the measurements and the breakdown voltage dropped to less than one tenth of the previous result. In Figures 5.2 and 5.3 you can see this type of irreversible breakthrough and big decrease of breakdown voltage. Only diodes in case type 1 and 2 modules experienced this type of big decrease of breakdown voltage. 33 % of case type 1 and 11 % of case type 2 modules had at least one diode that

got severely damaged and experienced a big decrease of the breakdown voltage value. This happened in both new and used modules.

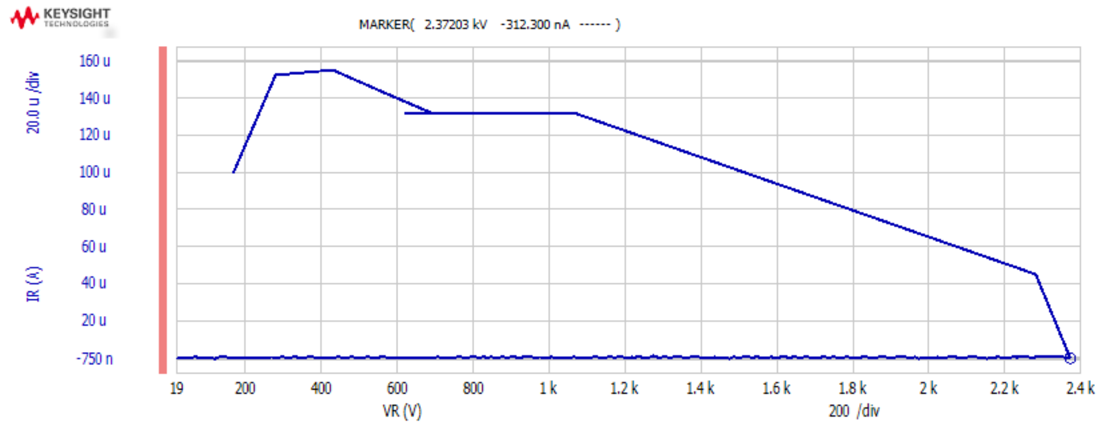

Figure 5.2. Irreversible breakthrough happened during measurements. The diode was first able to withstand a reverse voltage of 2370 V, but when the breakdown happened the voltage started to drop.

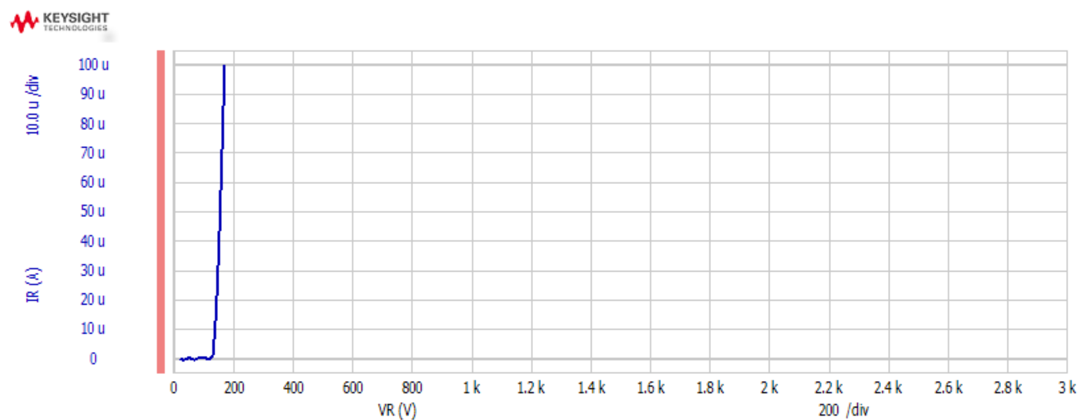

Figure 5.3. The breakdown voltage measurement curve of a diode that has suffered an irreversible breakthrough in the previous measurement (Figure 5.2). The breakdown voltage of the measured diode has dropped to under 200 V, which means that there is a short circuit.

Case type 2 modules had a significant amount of diodes that showed gradual decrease of breakdown voltage during the subsequent measurements. The breakdown voltages decreased at least 40 V during the three measurements in at least one diode in 70 % of case type 2 modules. This type of gradual decrease happened mostly in case type 2 modules as only one case type 1 and no case type 3 modules experience this type of

decrease in the breakdown voltages. Some diodes also showed slight increase of breakdown voltage. 10 % of case type 1 and 22 % of case type 2 modules had at least one diode showing at least 40 V increase during the subsequent measurements. Case type 3 modules did not have any increase or decrease during the measurements.

Case type 1 and 2 had significant variation in the breakdown voltage values. Even diodes inside the same module had hundreds of volts differences between one another. Case type 1 modules had diodes with breakdown voltages ranging between 2000 V and 2500 V and diodes with breakdown voltages from 0 V to 800 V. Case type 1 had no correlation between the breakdown voltage values and weather the module was used or not. Case type 2 had the most variation in the breakdown voltages and the breakdown voltage values of new and used modules had differences. The diodes in new case type 2 modules had breakdown voltages between 1500 V and 2100 V. Diodes in used case type 2 modules had breakdown voltages between 1000 V and 2100 V and diodes with breakdown voltages from 0 V to 200 V. In case type 3 modules all diodes had a breakdown voltage value of more than 2400 V up to over 2800 V regardless of whether the module had been used or not. The highest measured breakdown voltages for each diode are presented in Tables 5.3 and 5.4.

Table 5.3. The highest measured breakdown voltages $U_{br,max}$ for each diode. The results of all new unused rectifier modules N1-N35 are presented in this table.

Name	Case type	Ubr,max L1-	Ubr,max L2-	Ubr,max L3-	Ubr,max L1+	Ubr,max L2+	Ubr,max L3+
N1	1	2420	2340	2380	2380	2410	2380
N2	1	2390	2440	2400	2360	2490	2390
N3	1	2380	2280	2390	2340	2330	2400
N4	1	2370	2440	2410	2400	2400	2450
N5	1	2430	2320	2330	2400	2380	2410
N6	1	2360	2310	2220	2310	2400	2350
N7	1	2470	2380	2460	2460	2380	2450
N8	2	1960	2020	1820	1950	1820	1680
N9	2	2030	2060	2050	1740	1960	1840
N10	3	2550	2560	2530	2600	2580	2560
N11	3	2720	2710	2700	2700	2710	2580
N12	3	2660	2510	2550	2470	2590	2600
N13	3	2720	2710	2730	2730	2710	2700
N14	3	2820	2800	2810	2750	2760	2700
N15	3	2770	2750	2790	2760	2810	2780
N16	1	2370	2380	2370	2400	2410	2410
N17	1	2410	2420	2390	2360	2390	2440
N18	1	2400	2330	2370	2340	2360	2390
N19	1	2390	2430	2400	2010	2350	2310
N20	1	2390	2440	2350	2320	2460	2420
N21	2	1690	1790	1840	1650	1680	1860
N22	2	1910	1880	1830	1590	1680	1640
N23	2	1980	2030	1770	1800	1770	1780
N24	2	1760	2050	1970	1700	1950	1570
N25	2	2010	1980	1530	1810	1920	1770
N26	3	2680	2680	2690	2690	2670	2690
N27	3	2710	2710	2690	2690	2710	2650
N28	3	2690	2760	2770	2770	2780	2780
N29	3	2590	2630	2630	2650	2640	2680
N30	3	2760	2710	2720	2690	2640	2710
N31	3	2700	2740	2690	2710	2640	2710
N32	3	2670	2700	2700	2690	2690	2640
N33	3	2730	2710	2670	2700	2730	2720
N34	3	2610	2630	2630	2640	2640	2680
N35	3	2690	2680	2730	2690	2700	2690

Table 5.4. The highest measured breakdown voltages $U_{br,max}$ for each diode. The results of all used rectifier modules R11-R66 are presented in this table.

Name	Case type	$U_{br,max}$ L1-	$U_{br,max}$ L2-	$U_{br,max}$ L3-	$U_{br,max}$ L1+	$U_{br,max}$ L2+	$U_{br,max}$ L3+
R11	2	1560	1840	1620	1160	1170	1370
R14	1	180	330	360	120	380	350
R17	2	1490	1600	1390	1310	1390	1390
R19	2	1720	1720	1710	1320	1440	1340
R21	1	2460	2410	2460	2520	2420	2390
R22	2	1710	1580	1690	1030	1090	1090
R23	2	1710	1560	1700	1600	1490	1680
R24	2	1580	1600	1630	1450	1510	1620
R25	2	1320	1170	1540	1110	1130	1210
R26	2	1470	1500	1800	1250	1230	1190
R27	2	1400	1430	1390	1090	1070	1150
R28	2	1710	1480	1750	1500	1730	1630
R29	2	1810	1650	1540	1460	1620	1620
R30	2	1760	1680	1570	1510	1550	1540
R31	2	1540	1540	1480	1460	1560	1470
R32	2	2050	2020	2080	1430	1450	1560
R33	2	1730	1620	1850	1510	1760	1600
R34	2	1540	1750	1720	1680	1640	1600
R35	2	1600	1600	1530	1560	1720	1780
R36	2	1890	1860	1790	1200	1300	1290
R37	2	0	0	0	1500	1490	1490
R38	2	1900	1810	2060	1580	1600	1630
R39	2	1990	1940	2010	1650	1640	1630
R40	2	1680	1710	1650	1680	1710	1770
R41	2	2040	2040	2040	0	0	0
R42	2	0	0	0	1810	1810	1810
R43	2	0	1830	1810	1850	1760	1630
R44	2	1520	0	0	0	0	0
R45	2	0	1730	0	1680	1670	1680
R46	2	0	1120	0	1390	1380	1370
R47	2	1960	1920	1990	1710	1790	1760
R48	2	1910	2140	2140	1510	1640	1720
R49	1	2100	2100	2100	0	70	0
R50	1	2370	2380	2380	2380	2380	0
R51	1	2400	2390	10	0	10	0
R52	1	1840	20	20	20	20	0
R53	1	2400	2420	2400	2280	0	2350
R54	1	2190	2190	2180	2180	0	400
R55	1	2370	0	2270	2160	2370	410
R56	1	2250	2300	2300	2250	2270	2230
R57	1	2320	2440	2380	2510	2370	2200
R58	1	2460	2430	2490	2460	2500	2400
R59	1	2410	2410	2380	2460	2380	2430
R60	1	2240	2280	2250	2220	2210	2190
R61	1	2220	2250	2270	2290	2260	2220
R62	1	2240	2220	2200	2260	2210	2270
R63	1	2290	2240	2220	2230	2300	2280
R64	1	2220	2280	2250	2240	2220	2040
R65	3	2700	2710	2720	2740	2720	2690
R66	3	2780	2710	2720	2710	2710	2700

6 Examining the structure and materials of the modules

All three case types were examined to find out any structural differences that might explain the performance differences.

6.1 Possible materials inside the modules

The modules were expected to consist of chemical elements shown in Table 5.1. The table shows some of the chemical elements most commonly found in electronic components and their mass densities. For example copper was a possible materials for the conducting structures, epoxy was expected to be the case material, the diode chips were expected to be silicone and the rest were possible chemical elements in the solder or as some sort of protective structure. Lead is also in the table although it is one of the restricted substances of RoHS (Tukes, 2019). Lead is still commonly used in solders and components, and it is permitted to have 0,1 % restricted substances in a homogenous material (Tukes, 2019). The elements are chosen based on their price and properties. Properties such as hardness, brittleness, ductility, corrosion resistance, electrical conductivity, melting point and mass density are considered when choosing a suitable material (Gupta and Gupta, 2015).

Table 6.1. Possible chemical elements and substances inside the rectifier modules and their mass densities (Lenntech, 2019; Prospector, 2019; Wikipedia, 2019).

Chemical element or substance	Mass density [g/cm^3]
Air	0,0012
Epoxy	0,95−1,87
Silicon (Si)	2,33
Aluminum (Al)	2,7
Tin (Sn)	7,31
Nickel (Ni)	8,9
Copper (Cu)	8,96
Silver (Ag)	10,5
Lead (Pb)	11,35
Gold (Au)	19,3

6.2 X-ray imaging

X-ray imaging was used for finding out the internal structure of the rectifier modules. The data sheets of the diodes only provided a circuit diagram, but the implementation remained unknown. Using X-ray imaging it is possible to see which parts of the component have a higher mass density. Higher mass densities appear as lighter areas in the X-ray images.

X-ray images were taken of all the rectifier modules before and after the breakdown voltage measurements. The images revealed that there were three different inner structures used in the rectifier modules. The inner structures corresponded to the case type.

Case type 1 was from Diotec. The X-ray images of case type 1 rectifier modules showed a mesh pattern over the diode chips. From the X-ray images it was not possible to determine what caused the mesh pattern, but later it was revealed to be engravings on the copper parts around the diode chip. The mesh pattern existed only in case type 1 modules. Case type 1 modules had also anomalies such as voids, misaligned chips and inconsistent soldering. Some of case type 1 modules also showed a very narrow insulation between the minus pin and the phase pin next to it. X-ray images of all three case types are shown in Figure 6.1.

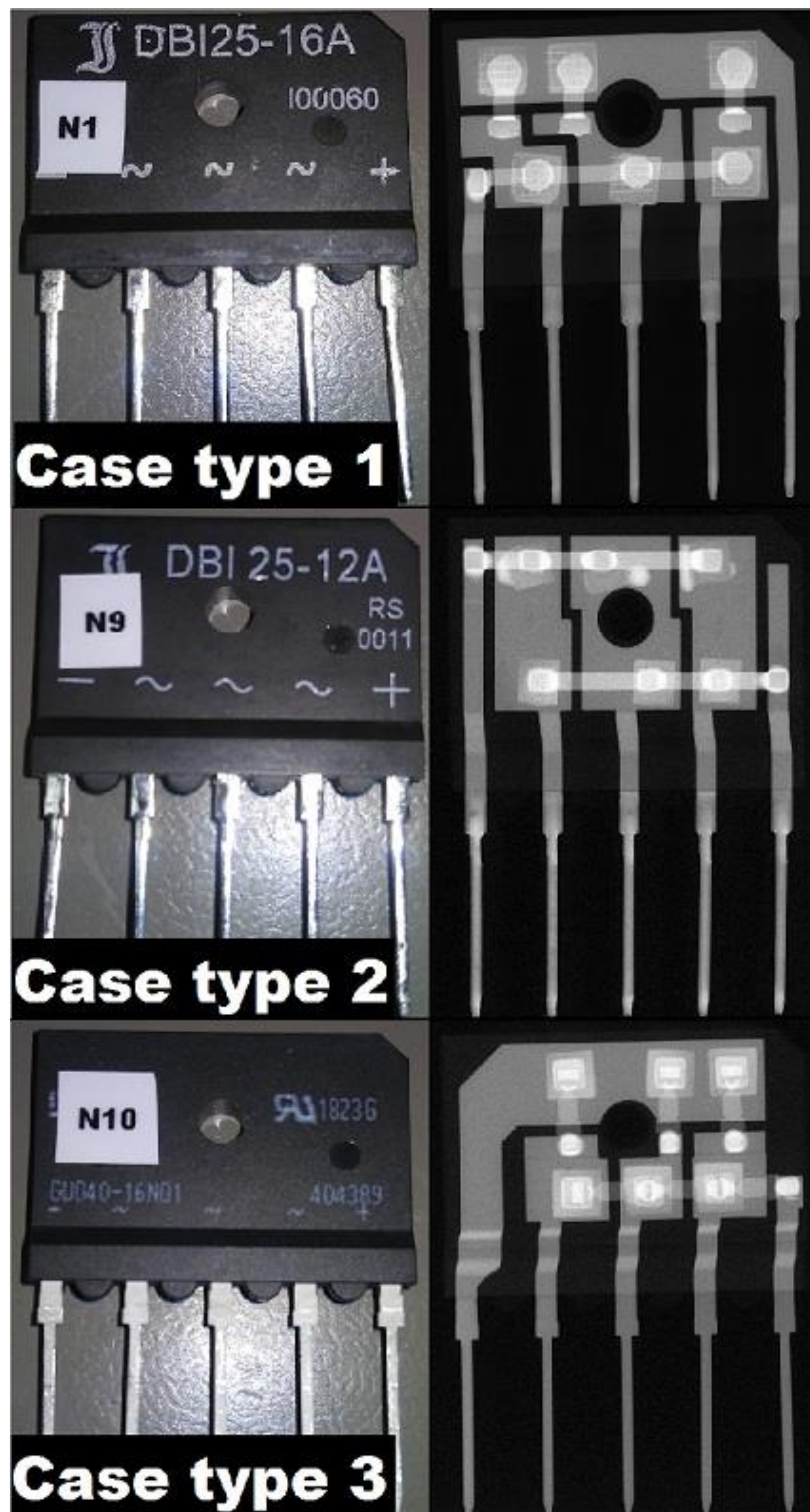

Figure 6.1. 2D X-ray images of all three case types.

Case type 2 was also from Diotec. This case type did not have the mesh pattern that the other case type from the same manufacturer had. This case type also had a bar connecting the diodes on both plus and minus sides, whereas case type 1 had a bar on only minus side. The way diodes were attached to other the conducting parts was different for case type 1 and case type 2. Case type 1 had a circular shape and case type 2 a square shape visible at each diode chip. Case type 2 modules also had voids, misaligned chips and inconsistent soldering. The number of voids in case type 2 modules was significantly lower than in case type 1 modules.

Case type 3 was from Ixys. Case type 3 modules had less voids than the other case types, but the inconsistent soldering was still visible. The chips were well aligned and there was not much disparity between case type 3 modules. Case type 3 modules had yet a different kind of attachment of diodes. There was no mesh visible in type 3 modules, but there were more layers and a more complex structure than in case type 1 and 2 modules.

The modules were X-ray imaged again after the breakdown measurements. Some modules experienced some sort of damage during the measurements and their breakdown voltages dropped significantly. The X-ray images were carefully inspected to find any signs of breakthrough. No visible changes could be found at least from this angle of imaging.

Since 2D images only give a very restricted view of the modules, also 3D X-ray imaging was used. Due to equipment availability, the 3D X-ray imaging could only be used on a couple of modules. The 3D imaging didn’t reveal any anomalies or signs of breakdown in the dielectric. It, however, did show that some of the silicon chips were badly damaged as shown in Figure 6.2.

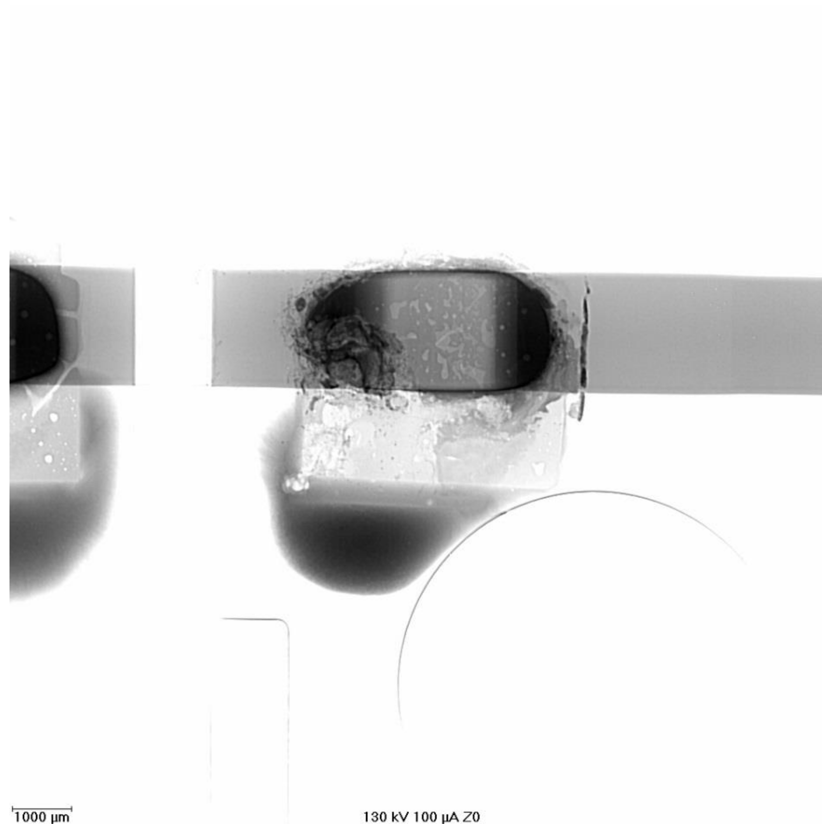

Figure 6.2. A badly damaged silicon chip on case type 2 module R44.

6.3 Destructive methods

Ten additional Ixys diode bridge rectifier modules were purchased for testing out different methods of opening the cases. Removing the epoxy case was attempted by dissolving and by melting. Some modules were also split to see the cross section.

Dissolving was attempted with dichloromethane and ethanol. Modules were left immersed in the chemicals and they were observed multiple times during the process. Dissolving with dichloromethane was carried out for 24 hours and dissolving with ethanol for two weeks. Neither one was able to dissolve the case even slightly. Sulfuric acid possibly could have melted the epoxy, but most probably it would have also dissolved the internal structures.

Melting the epoxy case was first attempted in an oven at 200 degrees Celsius. The temperature wasn’t high enough to affect the epoxy at all. Next the module was put to a

500 degrees Celsius hot oven. The epoxy case melted, but also the attachments inside melted and the module broke into pieces. The internal structure also got damaged and oxidized. The epoxy seemed to be infused with some sort of heat durable filler, possibly sand. That filler remained on the surface of the chips.

The internal structure could be examined also by splitting the modules and observing the cross section. One of each case type was cut in half with a wet disc cutter to see the cross section. The modules were cut in half so that also at least one diode was cut in half and the attachment of the diodes could be seen as marked on Figure 6.3. After cutting the modules in half, the cross section surface was ground by hand with a variable speed grinding/polishing machine and an 800 grit SiC abrasive paper to find the desired cross section. Then the cross section was polished using 1 µm diamond spray.

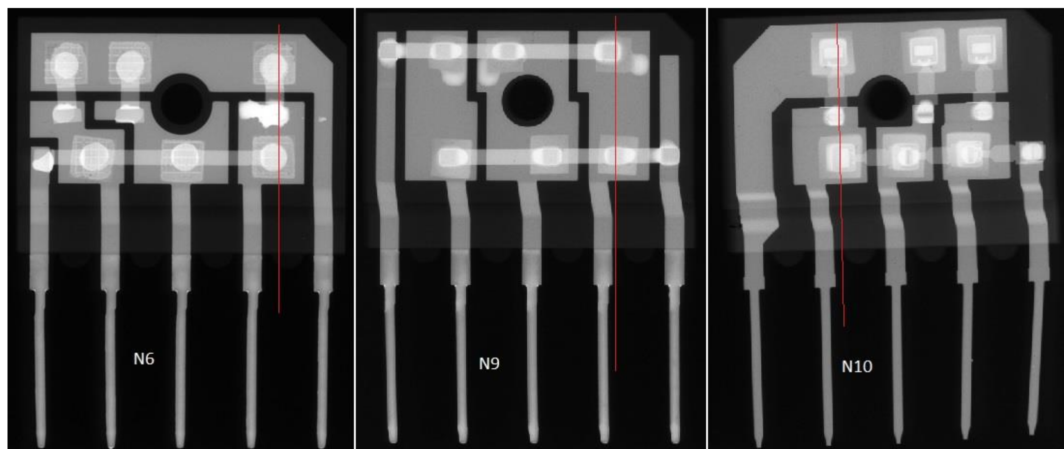

Figure 6.3. One of each case type rectifier module was cut to see the cross section. The location of the cut was chosen so that also two diodes were cut in half as marked with red lines.

Cutting and grinding the modules revealed that the mesh patterns in case type 1 modules were not caused by separate components. The mesh patterns in the X-ray images were actually caused by engravings on the copper as shown in Figure 6.4. All of the copper surfaces that were against a silicon chip had the engravings. Case types 2 and 3 did not seem to have engravings of any sort.

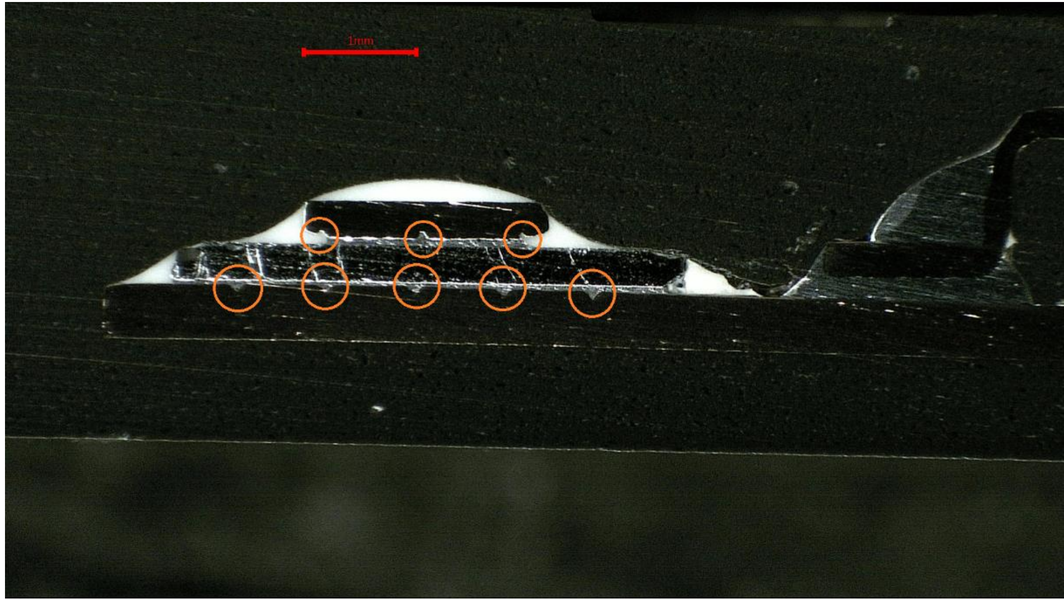

Figure 6.4. Optical microscope image of a case type 1 bottom row right side diode L3-. The cross section revealed that the mesh pattern was not an additional part, but it was caused by engravings on the copper. The engraving are marked with orange circles.

Case types 1 and 2 had two types of dielectric material used in the modules. Besides having black epoxy as the main case material, there was also a white dielectric used in the modules (Figure 6.5). The white dielectric covered the silicon chip junction areas and it was also used as an electrical insulator between the plus or minus rails and the phase planes. In case type 3 modules there was no white dielectric and the black epoxy casing filled the gap between the minus or plus rail and the phase planes (Figures 6.8 and 6.9). The thickness of insulation between live parts was also visibly bigger in case type 3 modules as show in Figure 6.6.

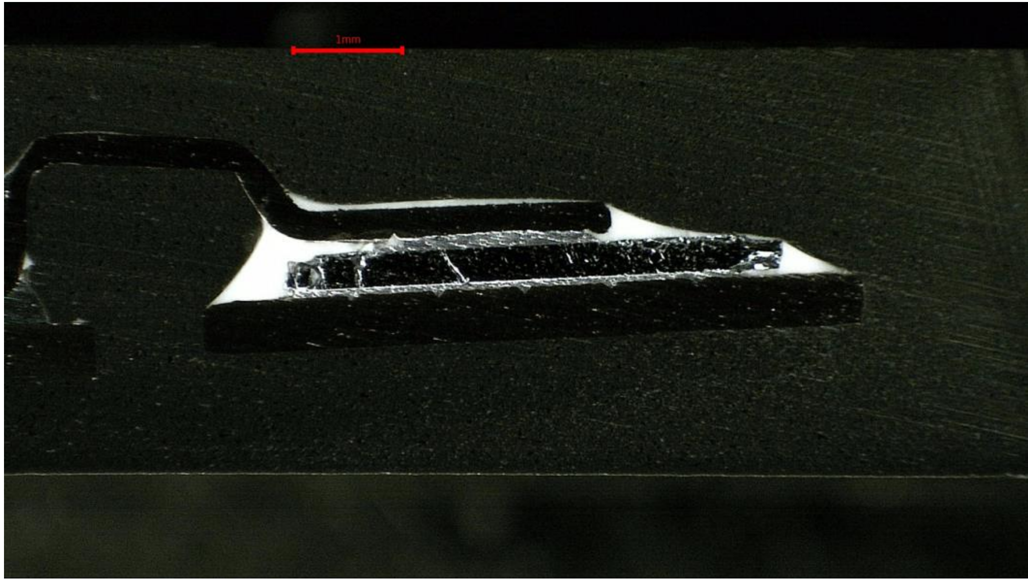

Figure 6.5. Case type 1 top row right side diode L3+. Case type 1 had a thick layer of solder on both sides of the diode chip and the junction area was covered with an unknown white substance.

Figure 6.6. The insulation gap was significantly bigger on case type 3 compared to case type 1 and 2. Case type 3 also had the same epoxy as on the case between the live parts whereas case types 1 and 2 had a white dielectric between the live parts. On left case type 3 and on the right case type 2 insulation thickness between live parts.

From the cross sections, it could be see that the thickness of the solder layers at junctions had differences. Case type 1 had the thickest layers of solder at junctions (Figure 6.5) and case type 2 had the thinnest layers (Figure 6.7). In case type 1 and 2 modules there were also visible air gaps at the junctions of different substances. Especially on the surfaces of the white dielectric, there were air gaps and small holes. The air gaps were confirmed by flushing the cross section surface with alcohol. The alcohol filled the gaps and then started to extrude out from the gaps forming drops on the cross section surface (Figure 6.7).

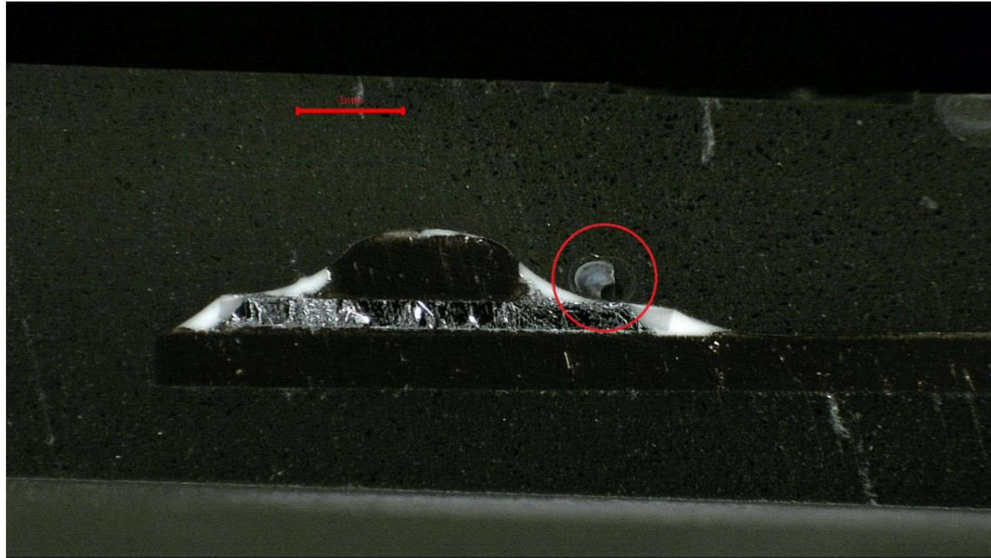

Figure 6.7. Case type 2 bottom right diode L3+. Case type 2 had thin solder layers and no "mesh". The edges of the white dielectric had air gaps especially in case type 2 modules. An alcohol drop gushing from an air gap is marked with a red circle.

The diodes of case type 1 and 2 modules also showed multiple cracks. The cracks however were probably caused by the cutting and grinding process. The modules were cut with the wet disc cutter from the middle of the diodes and they were not placed in a mold for support.

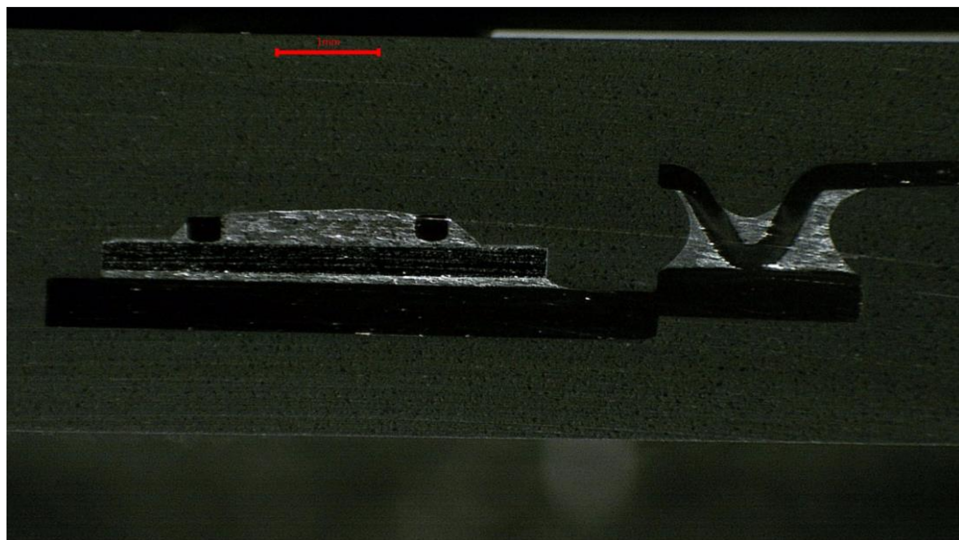

Figure 6.8. Case type 3 bottom left diode L1+. Case type 3 did not have any white dielectric inside and the structure was more complex than that of case types 1 and 2.

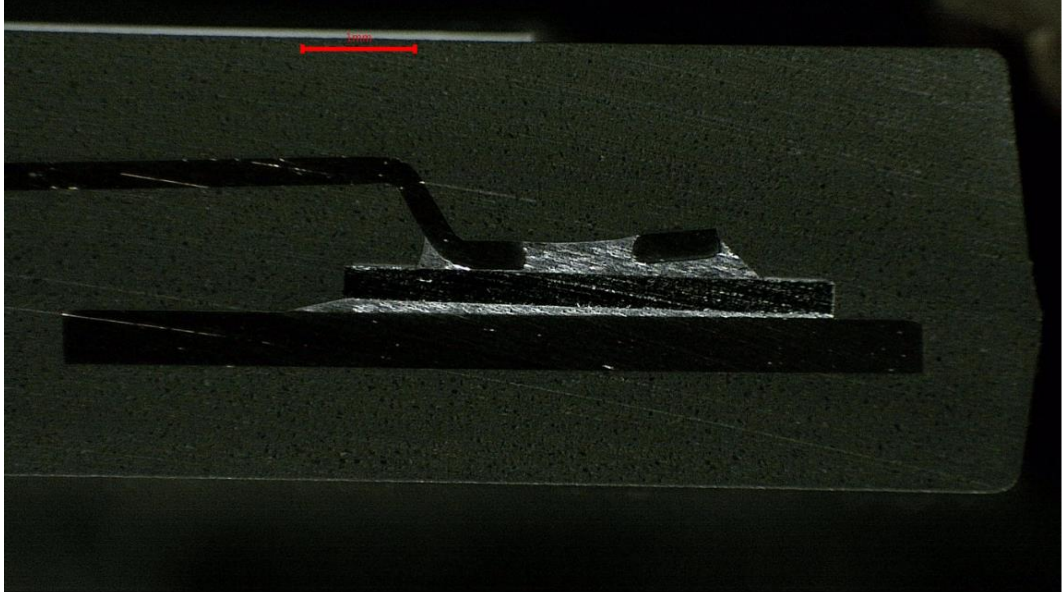

Figure 6.9. Top left diode L1-.

Module R50 was one of the case type 1 modules, which had a short circuit at one diode, more specifically diode L3+ at the top right corner. The 3D X-ray imaging showed some damage at the top left corner of the diode. The case was cut to get a piece with only the damaged diode. The piece with the diode was molded into epoxy for support and then it was carefully ground and polished to find the damaged corner of the diode. The diode had a crack in the middle (Figure 6.10) and one of its corners was badly molten (Figure 6.11). Since the piece was properly supported with the epoxy mold and it was slowly ground to the diode, it is very likely that the crack was not caused by the cutting or grinding process. The crack was most likely caused by mechanical stress in the manufacturing process or in use.

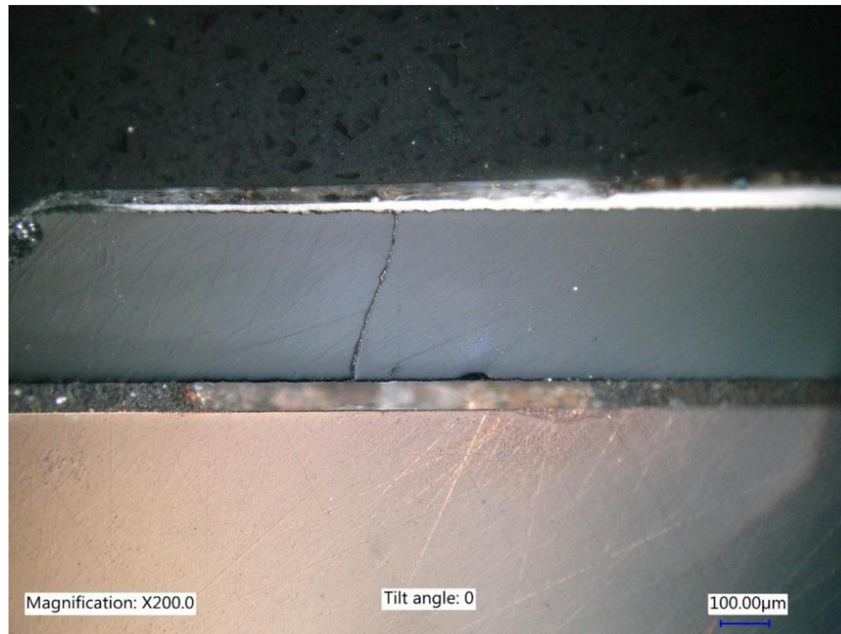

Figure 6.10. An optical microscope image of diode L3+ at the top right corner of module R50. The diode showed a short circuit at breakdown voltage measurements. The crack was probably caused by mechanical stress in the manufacturing process or in use.

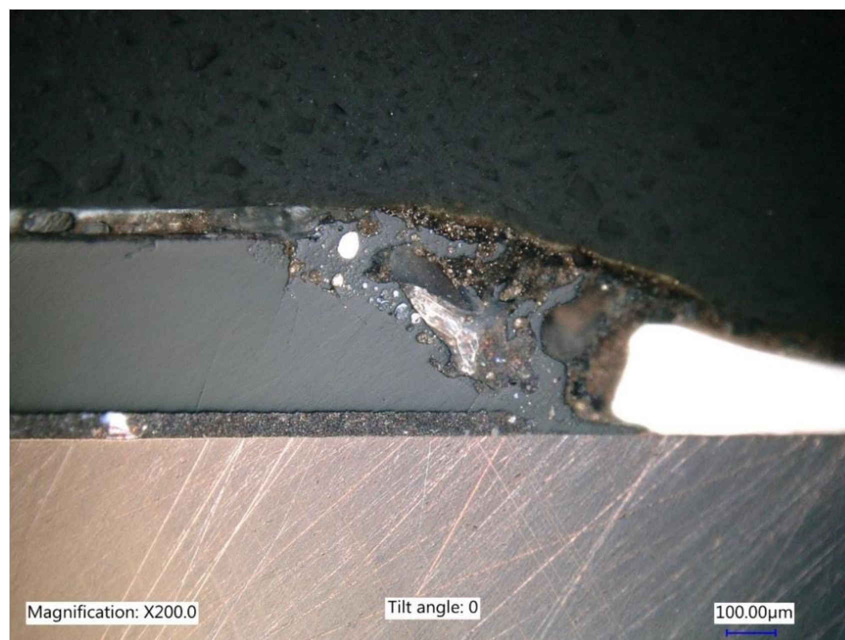

Figure 6.11. An optical microscope image of diode L3+ in case type 1 module R50. The diode showed a short circuit in the breakdown voltage measurements and the corner of the diode looked damaged in the 3D X-ray imaging. The cross section revealed severe heat damage in the corner. The heat damage was likely caused by excessive current.

The damage in the corner of diode L3+ in module R50 was clearly caused by heat. Heat can be caused by excessive current. In this case, it seemed to be a local hotspot since only one corner was molten. The 3D X-ray revealed heat damage in multiple other diodes that had a short circuit. The heat damage seemed to be either at a corner or at the edge of the diode chip. Hotspots can be caused by surface leakage, cracks or weak structure of the diode. The location of the heat damage suggests that the hotspots might be caused by surface leakage and/or cracks.

6.4 The chemical elements in the rectifier modules

A scanning electron microscope (SEM) and energy-dispersive X-ray spectroscopy (EDS) were used to analyze the cross sections of each case type. The aim was to identify the chemical elements in the modules. The cross sections of all three case types were examined.

Case type 1 was examined from a cross section of rectifier module N6. The SEM picture is shown in Figure 6.12. Case type 1 had two types of solder used inside it. The junctions connecting copper to copper had solder, which was mostly tin and only a couple percent lead. The junction connecting the diode chip to copper had solder, which was totally opposite – mostly lead and only a couple percent tin. The solder layers were clearly the thickest of all three case type modules. Case type 1 also had two types of copper used. The bigger copper planes on the bottom had a couple percent iron infused to the copper whereas the narrow rails connected on top of the diodes were pure copper. The diode chip was mostly pure silicon, but at the top edges it had a ring of aluminum-silicon-lead mixture, which was possibly a guard ring to prevent surface leakage (Mishra, 2005). In case type 1 modules, the diode chip and all of the copper parts were coated with a micrometer layer of nickel. The white dielectric surrounding the whole diode junction area appeared to be some sort of fine-gained epoxy consisting of silicon, oxygen and carbon as the chemical elements. The black epoxy had the same chemical element content, but a coarser consistency.

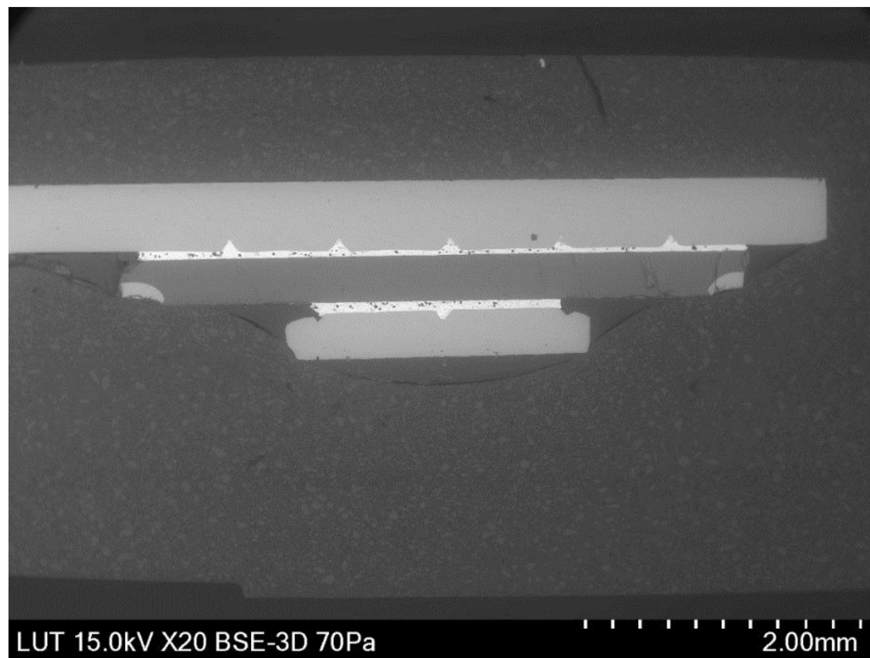

Figure 6.12. A SEM picture of case type 1 diode chip area. The cracks in this cross section were possibly caused by the cutting and grinding process. Notice the image is upside down.

Case type 2 was examined from a cross section of rectifier module N9. The SEM image of it is in Figure 6.13. Case type 2 had all of its internal bonds soldered with the same solder mixture. The solder was mostly lead and a couple percent tin. There was also a very small amount of copper mixed into the solder. The copper could also be from the copper parts and not in the solder originally. Case type 2 also had two types of copper used the same way as case type 1 had. The bigger copper planes on the bottom had a couple percent iron infused and the narrow rails were pure copper. Unlike case type 1, case type 2 didn't have any coating on the copper parts. The diode chip was pure silicon and it was coated with a micrometer layer of nickel. The diode chip also possibly had an extremely thin titanium coating. Case type 2 had the same two epoxies as case type 1: the white fine-grained epoxy covering the diode junction areas and the coarser black epoxy as the main case material.

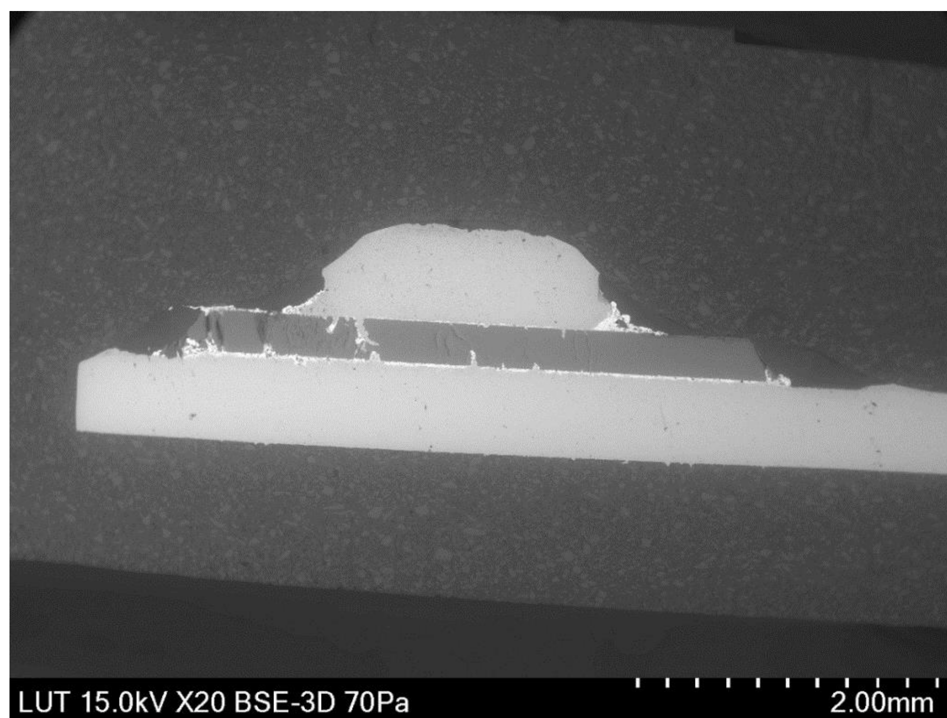

Figure 6.13. A SEM picture of case type 2 diode chip area. The cracks in the diode chip were possibly caused by the cutting and grinding process.

Case type 3 was examined from a cross section of rectifier module N10. The SEM image is shown in Figure 6.14. Case type 3 had two types of solder like case type 1, but the solder alloys weren't the same. The junctions connecting copper to copper and the junctions above the silicon chips had solder, which was almost pure lead. The junctions connecting the diode chip to the bigger copper plates below the chips had solder, which was mostly lead and a couple percent tin. The junctions below the chips had copper mixed into them as well. The soldering was done in such a manner that the copper and solder got clearly infused in the process and formed an intermetallic layer. This type of intermetallic layer makes the bond very strong, but the layer has to be thin since it is quite brittle (Fengshun et al., 2005). Unlike the other two case types, case type 3 had all of its copper parts made from pure uncoated copper. The diode chip was pure silicon and it had a nickel and titanium coating. An EDS mapping was done to a Cu-Si junction below the chip to get a proper understanding of the structure of the junction and the chemical elements present (Figure 6.15). Case type 3 had only one type of epoxy, which was the black coarse epoxy. No other dielectric materials were used in case type 3.

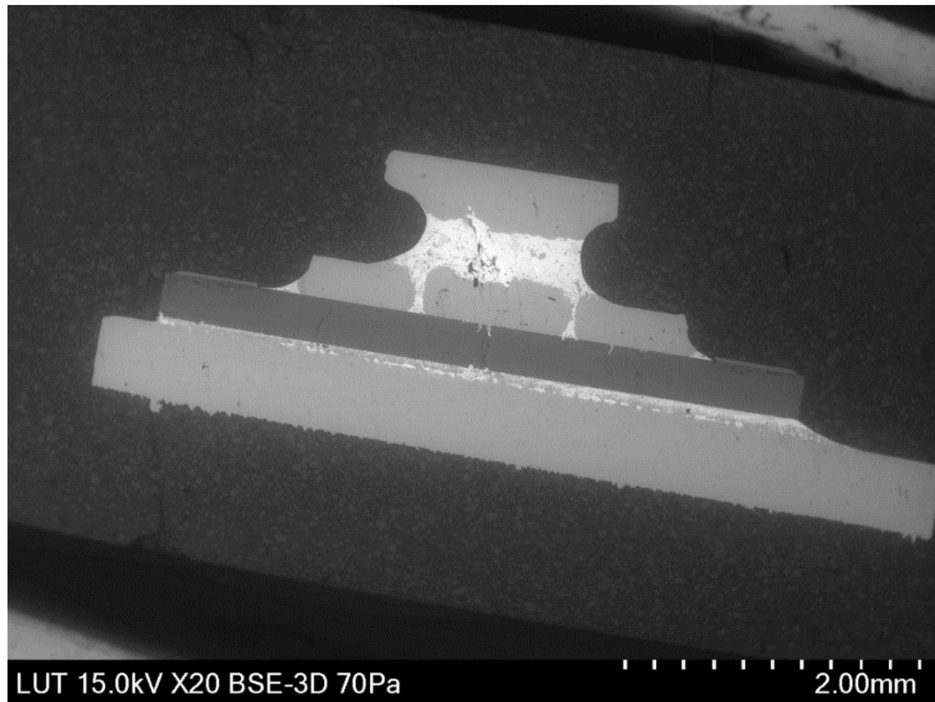

Figure 6.14. SEM picture of case type 3 diode chip area. A thick solder layer is utilized to get a wider gap between the live parts on either side of the diode.

All three case types also had small, less than 1 µm in diameter, nuggets of carbon in the solder. It is possible that they originated from the diamond polishing liquid in the polishing process, but they could also be part of the solder. There weren't any scratches caused by the rotating polishing disc and the nuggets were evenly spread in the solder, which suggests that they might have been a filler substance in the solders.

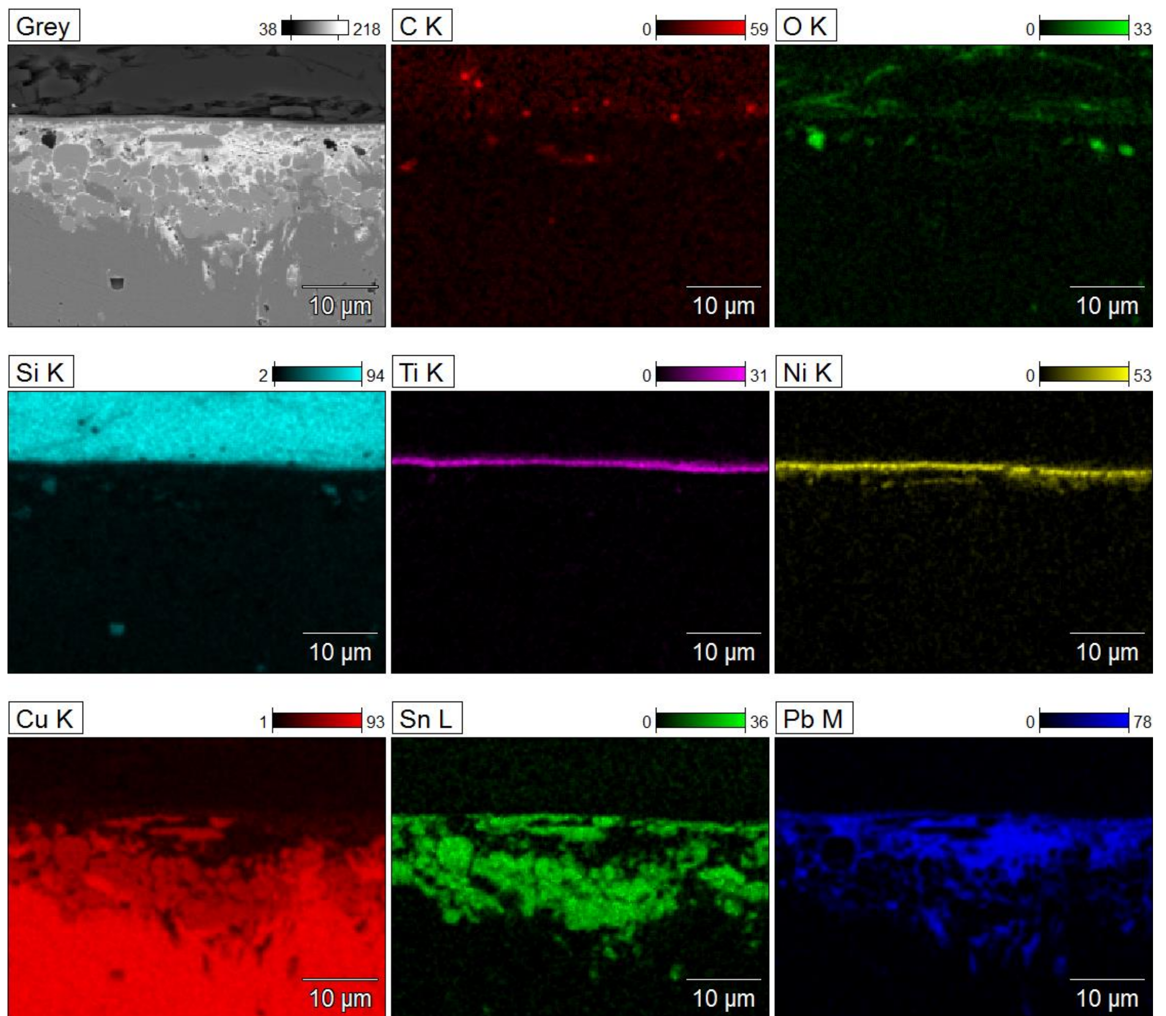

Figure 6.15. An EDS mapping was done to case type 3 Cu-Si hinge. Case type 3 had titanium and nickel on the surface of the silicon chip. The solder beneath the silicon chip was a mixture of tin and lead while the solder above the chip and at Cu-Cu junctions was almost pure lead. The solder beneath the chip was mixed with the copper.

7 Conclusions and discussion

The breakdown voltage measurements showed that case type 3 modules clearly outperformed case type 1 and 2 modules by having consistently high breakdown voltage values. Case type 3 had the biggest breakdown voltage values where as case type 2 had the lowest. Some unused case type 2 diodes didn't even reach the datasheet U_{RRM} value. In the breakdown voltage measurements, multiple case type 1 and some case type 2 modules suffered irreversible breakdown. A significant amount of case type 2 modules also showed gradual decrease of the breakdown voltage during measurements. Multiple used case type 1 and 2 modules had short circuits and the breakdown voltage had decreased to 0 V when used in the field. Used case type 2 field returns tended to have reduced values clearly below the datasheet values but not entirely short circuit. Used case type 3 modules performed as well as the new ones.

Several differences in structure were discovered. The 2D X-ray images revealed distinct differences in the metal structures and the EDS analysis unveiled differences in the chemical elements used in the modules. Differences in the structures of the three case types are shown in Table 7.1.

Dielectric weakness and breakdown was the initial presumption for the failure mechanism of case type 1 and 2 modules, but the 3D imaging didn't show any clear dielectric breakdown signs. The 3D imaging however did show clear heat damage in some case type 1 and 2 silicon chips. A couple of cracks were also found in case type 1 and 2 silicon chips. It is possible that the manufacturing process, other mechanical stress or heat stress causes small cracks to the silicon chips. These small cracks conduct more leakage current and cause local hotspots. Hotspots lead to degradation of the silicon chip and eventually to breakdown and severe heat damage.

Table 7.1. Differences in the structure of the three case types.

	Case type 1	**Case type 2**	**Case type 3**
Epoxy	Black rough epoxy as case material. White fine epoxy surrounding diode chip junctions and between live parts (bottom frame and rail).	Black rough epoxy as case material. White fine epoxy surrounding diode chip junctions and between live parts (bottom frame and rail).	Black rough epoxy as case material and as dielectric between live parts. No white epoxy.
Insulation	Dielectric thickness between live parts (bottom plate and rail) about 0,5 mm.	Dielectric thickness between live parts (bottom plate and rail) about 0,5 mm.	Dielectric thickness between live parts (bottom plate and rail) more than 1 mm.
Silicon chips	A thin layer of nickel coating the silicon chip. A "ring" of aluminium-silicon-lead mixture at the top edges of the silicon chip.	A thin layer of nickel coating the silicon chip. Possibly also a very small amount of titanium coating the silicon or in the solder connecting the silicon chip to the copper.	A thin layer of nickel and titanium coating the silicon chip.
Copper structures	The bigger copper plates (the main frame on the bottom) were infused with a couple of percents iron and the smaller copper parts (rails above diodes) were pure 100% copper. All copper parts were coated with a thin layer of nickel. The copper parts at Cu-Si joints had a mesh pattern engraved in them.	The bigger copper plates (the main frame on the bottom) were infused with a couple of percents iron and the smaller copper parts (rails above diodes) were 100% pure copper. No coating and no mesh pattern engraved.	All copper parts (the main frame on the bottom and rails above diodes) were 100% pure copper. No coating and no mesh pattern engraved.
Solder	Cu-Cu joints had solder which was mostly (>90%) tin and some lead. Cu-Si joints had solder which was mostly (>80%) lead and some tin. Solder layers in case type 1 were clearly the thickest of the three case types.	All solder was mostly lead with some tin. At some joints copper from the structures was also mixed into the solder.	Solder above the silicon chips at Si-Cu joits and at Cu-Cu joints was almost pure lead. Solder beneath the silicon chips at Cu-Si joints was mostly lead with some tin. Especially at the bottom Cu-Si joint the copper had melted and mixed into the solder.

Another possibility, besides cracks, is that the hotspot and breakthrough occurs at the edge of the diode. The diodes of case type 1 and 2 were covered with white epoxy and there were multiple air pockets found between the epoxy and diode. These air pockets enable treeing and breakthrough from the edge of the diode. The 3D X-ray imaging also revealed severe heat damage at the edges and corners of diodes that had a very low

breakdown voltage (short circuit). This type of heat damage never occurred in the middle of the diode. However, also cracks most often start from the edge of the diode.

In either case, the problem of Diotec rectifier modules originates from the manufacturing phase. The structure or the assembling method leads to uneven current distribution across the surface of the diode and hotspots. The ultimate result is breakdown, heat damage and, eventually, short circuit.

The poor availability of different imaging options made it difficult to figure out the phenomena happening inside the modules and to pinpoint the exact spots where the breakdowns happened. Finding out the breakdown points would have been possible with lock-in thermography. Lock-in thermography might also have revealed possible hotspots in modules with only slightly decreased performance values and breakdown voltages. Unfortunately, LIT equipment was not available and thus could not be used.

The availability of 3D X-ray imaging right from the beginning of the research would have also helped with understanding the phenomena. The first assumptions were that deterioration and breakdowns might happen in the epoxy insulation. Eventually 3D X-ray imaging showed no signs of deterioration or breakdowns in the insulation. Besides proving the previous assumption wrong, 3D X-ray imaging was easily able to uncover clear damage in the diode chips themselves.

References

Andersson, C., Kristensen, O., Miller, S., Gloor, T. and Iannuzzo, F. 2018. "Lock-in Thermography Failure Detection on Multilayer Ceramic Capacitors After Flex Cracking and Temperature–Humidity–Bias Stress." *IEEE Journal of Emerging and Selected Topics in Power Electronics*, vol. 6, no. 4, pp. 2254-2261.

Artyukov, I. A., Popov, N. L. and Vinogradov, A. V. 2018. "Spectrally Selective Soft X-ray Microscopy in Studies of Biological Objects." *2018 International Conference Laser Optics (ICLO)*, St. Petersburg, pp. 522-522.

Barth, M., Schubert, F. and Koehler, B. 2008. "Where X-ray imaging fails - delamination, crack, and micro-pore detection using ultrasonic reflection tomography in a scanning acoustic microscope." *2008 IEEE Nuclear Science Symposium Conference Record*, Germany, pp. 577-581.

Bernard, P. A. and Gautray, J. M. 1991. "Measurement of dielectric constant using a microstrip ring resonator." *IEEE Transactions on Microwave Theory and Techniques*, vol. 39, no. 3, pp. 592-595.

Champion, J.V., Dodd, S.J. and Vaughan, A.S. 2001. "Polymers, Electrical Breakdown of." *Encyclopedia of Materials: Science and Technology*, 2nd edition. Elsevier. Pp. 7649-7653. ISBN 978-0-08-043152-9.

Copper Development Association (CDA). 2019. "A Home DC Network." [Online] *https://copperalliance.org.uk.* URL: https://copperalliance.org.uk/about-copper/applications/home-electrical-systems/home-dc-network/ [Accessed 28 August 2019]

Diotec Semiconductor AG. 2017. "DBI25-08A ... DBI25-18A Three Phase Bridge Rectifier Dreiphasen-Brückengleichrichter." Version 2017-12-06.

E. M. S. 2014. “BREAKDOWN in SOLID DIELECTRICS” *Benha University, Faculty of Engineering at Shoubra, Electrical Engineering Department, High Voltage Engineering.* [Online] URL: http://www.bu.edu.eg/portal/uploads/Engineering,%20Shoubra/Electrical%20Engineering/3103/crs-8705/Files/BREAKDOWN%20in%20SOLID%20DIELECTRICS1.pdf [Accessed 10 June 2019]

EEEGUIDE. “Breakdown of Solid Dielectrics in Practice.” [Online] *Eeeguide.com.* URL: http://www.eeeguide.com/breakdown-of-solid-dielectrics-in-practice/ [Accessed 10 June 2019]

Fengshun, W., Yanxiang, H., Yiping, W., Bing, A. and Jinsong, Z. 2005. "The growth behavior of intermetallic compound layer at solder/Cu joint interface during soldering." *2005 6th International Conference on Electronic Packaging Technology*, Shenzhen, pp. 355-359.

Guarnieri, M. 2018. "Solidifying Power Electronics [Historical]." *IEEE Industrial Electronics Magazine*, vol. 12, no. 1, pp. 36-40.

Guo, H., Chen, Y., Geng, C. and Yue, C. 2018. "Mechanical and dielectric properties of polyether sulfone/epoxy resin — Bismaleimide composites." *2018 12th International Conference on the Properties and Applications of Dielectric Materials (ICPADM)*, Xi'an, pp. 270-274.

Gupta, K.M. and Gupta, N. 2015. “Advanced Electrical and Electronics Materials: Processes and Applications.” *Advanced Materials Series.* Scrivener Publishing. ISBN 9781118998359.

Heid, T., Fréchette, M. and David, E. 2013. "Dielectric properties of epoxy/POSS composites." *2013 Annual Report Conference on Electrical Insulation and Dielectric Phenomena*, Shenzhen, pp. 751-755.

IXYS. 2013. “Standard Rectifier 3~ Rectifier Bridge Part number GUO40-16NO1.”

IXYS. 2016. “High Voltage Standard Rectifier 3~ Rectifier Bridge Part number DNA40U2200GU.”

Keysight Technologies. 2019. “Keysight B1505A Power Device Analyzer/ Curve Tracer Data sheet.” Published in USA, June 7, 2019, 5990-3853EN.

Khan, H., Amin, M., Ali, M., Iqbal, M. and Yasin, M. 2017. “Effect of Micro/Nano-SiO2 on Mechanical, Thermal and Electrical Properties of Silicone Rubber, Epoxy and EPDM Composites for Outdoor Electrical Insulations.” *Turkish Journal of Electrical Engineering and Computer Sciences*, vol. 25, no. 2, pp. 1426-1435.

Klampar, M., Spohner, M., Skarvada, P., Dallaeva, D., Kobrtck J. and Liedermann, K. 2013. "Dielectric properties of epoxy resins with oxide nanofillers and their accelerated ageing." *2013 IEEE Electrical Insulation Conference (EIC)*, Ottawa, ON, pp. 286-290.

Lenntech. 2019. “Chemical elements listed by density.” [Online] *lenntech.com.* URL: https://www.lenntech.com/periodic-chart-elements/density.htm [Accessed 1 September 2019]

Liu, X., Li, Z., Miraldo, P., Zhong, K. and Shi, Y. 2016. "A Framework to Calibrate the Scanning Electron Microscope Under Variational Magnifications." *IEEE Photonics Technology Letters*, vol. 28, no. 16, pp. 1715-1718.

Mishra, V., Srivastava, V. and Kataria, S. 2005. ”Role of guard rings in improving the performance of silicon detectors.” *Pramana – journal of physics*. Indian Academy of Sciences, vol. 65, no. 2, pp. 259–272.

National Technical Systems. 2019. “Analysis via Scanning Electron Microscopy / Energy Dispersive X-Ray Spectroscopy (SEM/EDS).” [Online] *Nts.com.* URL: https://www.nts.com/services/testing/electrical/sem-eds-analysis/ [Accessed 15 August 2019]

Obreja, V. V. N. and Obreja, A. C. 2010. "Breakdown of semiconductor devices and influence of the interface from passivated termination," *CAS 2010 Proceedings (International Semiconductor Conference)*, Sinaia, pp. 495-498.

Obreja, V. V. N., Codreanu, C., Poenar, D. and Buiu, O. 2005. "Semiconductor PN junction failure at operation near or in the breakdown region of the reverse I-V characteristic." *Proceedings of the 12th International Symposium on the Physical and Failure Analysis of Integrated Circuits, 2005. IPFA 2005.* Singapore, pp. 200-204.

Pham Tu Quoc, S., Cheymol, G. and Semerok, A. 2013. "Phase lock-in thermography for metal walls characterization." *2013 3rd International Conference on Advancements in Nuclear Instrumentation, Measurement Methods and their Applications (ANIMMA)*, Marseille, pp. 1-4.

Prospector. 2019. “Epoxy Typical Properties Generic Epoxy.” [Online] *ulprospector.com.* URL: https://plastics.ulprospector.com/generics/13/c/t/epoxy-properties-processing [Accessed 1 September 2019]

Qamar, A., Tanner, P., D. V. Dao, D. V., Phan, H. and Dinh, T. 2014. "Electrical Properties of p-type 3C-SiC/Si Heterojunction Diode Under Mechanical Stress." *IEEE Electron Device Letters*, vol. 35, no. 12, pp. 1293-1295.

Rashid, M. H. 2018. “Power Electronics Handbook.” 4th ed. Saint Louis: Elsevier Science.

Semiconductor Technology. 2019. “Fundamentals: Conductors – Insulators – Semiconductors.” [Online] *halbleiter.org.* URL: https://www.halbleiter.org/en/fundamentals/conductors-insulators-semiconductors/ [Accessed 1 September 2019]

Semmens, J. E. 2019. "Acoustic Micro Imaging and X-Ray Analysis for More Thorough Evaluation of Microelectronic Devices." *2019 Pan Pacific Microelectronics Symposium (Pan Pacific)*, Kauai, HI, USA, pp. 1-4.

Song, M., Cao, K. N., Wang, D. D., Yang, X. and Wei, B. 2014. "AC and Impulse Dielectric Strength of Polymer Materials Under Tensile Stress at 77 K." *IEEE Transactions on Applied Superconductivity*, vol. 24, no. 5, pp. 1-4, Art no. 0601304.

Sylvester, Y. et al. 2013. "3D X-Ray microscopy: A non destructive high resolution imaging technology that replaces physical cross-sectioning for 3DIC packaging." *ASMC 2013 SEMI Advanced Semiconductor Manufacturing Conference*, Saratoga Springs, NY, pp. 249-255.

Tech Briefs Media Group. 2014. "Evaluating Electrically Insulating Epoxies." [Online] *Techbriefs.com.* URL: https://www.techbriefs.com/component/content/article/tb/features/articles/20977 [Accessed 15 May 2019]

Tipler, P. 1987. "College physics." New York, NY: Worth Publishers. 932 pages. ISBN 10: 0879012684.

Tukes. 2019. "Vaaralliset aineet sähkö- ja elektroniikkalaitteissa – RoHS." [Online] *tukes.fi.* URL: https://tukes.fi/tuotteet-ja-palvelut/sahkolaitteet/sahkolaitteiden-vaatimuksia/vaaralliset-aineet-sahko-ja-elektroniikkalaitteissa-rohs [Accessed 1 September 2019]

Veena, M. G., Renukappa, N. M., Shivakumar, K. N. and Seetharamu, S. 2012. "Study of interface behavior on dielectric properties of epoxy-silica nanocomposites." *2012 IEEE 10th International Conference on the Properties and Applications of Dielectric Materials*, Bangalore, pp. 1-4.

Vorob'ev, G., Ekhanin, S. and Nesmelov, N. 2005. "Electrical breakdown in solid dielectrics." *Physics of the Solid State,* vol. 47, issue 6, pp. 1083-1087.

Wang, Y., Peng, Z., He, S., Zhu, B., Zhang, Y. and Chen, J. 2018. "Research on Failure Mechanism of Chip Welding Voids for Power Semiconductor Devices." *2018 IEEE International Symposium on the Physical and Failure Analysis of Integrated Circuits (IPFA)*, Singapore, pp. 1-4.

Wikipedia. 2019. "Density of air." [Online] *wikipedia.org.* URL: https://en.wikipedia.org/wiki/Density_of_air [Accessed 1 September 2019]

Zavattoni, L., Lesaint, O., Gallot-Lavallée, O. and Reboud, J. L. 2013. "Influence of water content and temperature on conduction and field on an Alumina/epoxy insulator." *2013 IEEE International Conference on Solid Dielectrics (ICSD)*, Bologna, pp. 246-249.

Zheng, H., Rowland, S. M., Iddrissu, I. and Lv, Z. 2017. "Electrical treeing and reverse tree growth in an epoxy resin." *IEEE Transactions on Dielectrics and Electrical Insulation*, vol. 24, no. 6, pp. 3966-3973.

Appendix 1. The difference between the first and the last breakdown voltage measurement result for each diode in the new unused rectifier modules.

Name	Case type	ΔU_{br} L1-	ΔU_{br} L2-	ΔU_{br} L3-	ΔU_{br} L1+	ΔU_{br} L2+	ΔU_{br} L3+
N1	1	10	0	0	0	10	20
N2	1	-1630	0	0	0	0	0
N3	1	0	0	0	0	0	-10
N4	1	-2240	-10	-2410	0	0	0
N5	1	0	-10	0	0	0	0
N6	1	0	0	-90	10	-1760	-10
N7	1	-1970	-10	-10	10	-1910	0
N8	2	-10	-10	-10	90	-30	-120
N9	2	0	-10	-10	-30	-10	-40
N10	3	-10	0	0	-10	0	-10
N11	3	0	-10	0	-10	-10	-10
N12	3	-10	0	0	-10	0	-10
N13	3	0	-10	0	-10	0	-20
N14	3	0	0	-10	-10	0	-10
N15	3	0	-10	-10	0	0	-10
N16	1	0	0	0	0	0	0
N17	1	0	0	0	0	0	0
N18	1	0	0	0	0	0	0
N19	1	-10	0	0	90	0	0
N20	1	0	0	0	0	60	0
N21	2	-40	-20	-20	-10	10	10
N22	2	0	-10	-50	10	-10	0
N23	2	-70	0	-110	-10	0	0
N24	2	-130	-10	0	0	0	0
N25	2	10	0	60	0	0	10
N26	3	-10	0	-10	0	0	0
N27	3	-10	0	-10	0	0	0
N28	3	0	0	0	0	0	0
N29	3	-10	-10	0	0	0	-10
N30	3	0	0	0	0	0	0
N31	3	0	10	-10	-10	-10	-10
N32	3	-10	0	-10	0	10	0
N33	3	0	0	0	-10	0	0
N34	3	-20	-10	0	0	0	0
N35	3	0	0	-10	-10	0	0

Appendix 2. The difference between the first and the last breakdown voltage measurement result for each diode in the unused field returned rectifier modules.

Name	Case type	ΔU_{br} L1-	ΔU_{br} L2-	ΔU_{br} L3-	ΔU_{br} L1+	ΔU_{br} L2+	ΔU_{br} L3+
R11	2	-130	-60	-130	-40	-50	-50
R14	1	0	0	0	0	0	0
R17	2	10	-100	-80	-20	-40	-10
R19	2	40	40	70	0	-60	40
R21	1	-10	0	0	0	0	0
R22	2	-30	-50	-110	-30	-70	-70
R23	2	-50	-70	-80	10	-20	10
R24	2	-80	-150	-120	-60	-20	20
R25	2	-10	-40	-70	-10	30	40
R26	2	-90	-120	-120	-30	-40	-40
R27	2	-60	-50	-10	10	60	20
R28	2	-60	-30	-40	0	10	10
R29	2	-60	-70	-80	-100	-30	-10
R30	2	-80	-1530	-90	0	10	40
R31	2	-40	-70	-40	0	10	-10
R32	2	-60	-20	-10	-10	-30	-40
R33	2	-150	-90	0	20	10	20
R34	2	-40	-40	-60	10	70	0
R35	2	-80	-80	-50	0	10	30
R36	2	-30	-110	-70	-50	-50	-60
R37	2	0	0	0	10	0	0
R38	2	-20	-30	0	20	0	20
R39	2	-10	-60	0	40	10	0
R40	2	-60	-20	-70	-10	0	30
R41	2	0	0	0	0	0	0
R42	2	0	0	0	30	0	0
R43	2	0	0	-10	-30	10	10
R44	2	-1520	0	0	0	0	0
R45	2	0	-1530	0	-10	0	10
R46	2	0	-1120	0	0	-10	-10
R47	2	0	0	10	30	10	0
R48	2	0	0	-10	10	-20	-20
R49	1	-10	0	0	0	-30	0
R50	1	-10	0	10	0	-10	0
R51	1	-2390	-2380	0	0	0	0
R52	1	-1820	0	0	0	0	0
R53	1	-10	0	0	-2160	0	0
R54	1	0	-10	0	0	0	-220
R55	1	0	0	-2220	-2160	-2070	40
R56	1	0	0	0	0	0	0
R57	1	0	0	0	0	0	10
R58	1	0	0	0	-10	0	0
R59	1	0	-2300	0	0	0	0
R60	1	0	0	0	0	0	0
R61	1	0	0	0	0	-10	0
R62	1	0	0	0	-10	0	0
R63	1	0	0	0	0	0	0
R64	1	0	0	0	0	0	-10
R65	3	0	-10	0	-10	-10	0
R66	3	-10	0	0	-10	-10	0